EUROPEAN ORGANIZATION FOR NUCLEAR RESEARCH (CERN)

CERN-EP-2021-027
LHCb-PAPER-2020-046
March 11, 2021

Precise measurement of the f_s/f_d ratio of fragmentation fractions and of B_s^0 decay branching fractions

LHCb collaboration†

Abstract

The ratio of the B_s^0 and B^0 fragmentation fractions, f_s/f_d, in proton-proton collisions at the LHC, is obtained as a function of B-meson transverse momentum and collision centre-of-mass energy from the combined analysis of different B-decay channels measured by the LHCb experiment. The results are described by a linear function of the meson transverse momentum, or with a function inspired by Tsallis statistics. Precise measurements of the branching fractions of the $B_s^0 \to J/\psi\phi$ and $B_s^0 \to D_s^-\pi^+$ decays are performed, reducing their uncertainty by about a factor of two with respect to previous world averages. Numerous B_s^0 decay branching fractions, measured at the LHCb experiment, are also updated using the new values of f_s/f_d and branching fractions of normalisation channels. These results reduce a major source of systematic uncertainty in several searches for new physics performed through measurements of B_s^0 branching fractions.

Submitted to Phys. Rev. D

†Authors are listed at the end of this paper.

Measurements of branching fractions of B_s^0 meson decays are sensitive tools to test the Standard Model (SM) of particle physics. They often require knowledge of the B_s^0 production rate. To avoid uncertainties related to the b-hadron production cross-section and integrated luminosity, and to partly cancel those related to detection efficiencies, at hadron colliders the B_s^0 branching fractions are often measured relative to other B-meson decay channels. In the absence of any precisely known B_s^0 branching fraction, most measurements are normalised to B^+ or B^0 meson decays, and thus require the ratio of their fragmentation fractions as input. The fragmentation fractions, denoted as f_u, f_d, f_s, and f_{baryon}, are the probabilities for a b quark to hadronise into a B^+, B^0, B_s^0 meson or a b baryon.[1] These fractions include contributions from intermediate states decaying to the aforementioned hadrons via the strong or electromagnetic interaction.

The b-hadron fragmentation fractions in proton-proton (pp) collisions at the Large Hadron Collider (LHC) energies are in general different from those measured at e^+e^- colliders [1–4] or in $p\overline{p}$ collisions at the Tevatron [5], with which they were previously averaged [6, 7]. The ratios of fragmentation fractions are found to depend on kinematics, in particular on the b-hadron transverse momentum with respect to the beam direction (p_{T}); the dependence on the b-hadron pseudorapidity (η) has also been studied, but not found to be significant [5, 8, 9]. The ratio of fragmentation fractions f_s/f_u has also been shown to depend on the pp collision centre-of-mass energy, $\sqrt{s}$ [10]. In the following, $f_u = f_d$ is assumed to hold due to isospin symmetry.

The $B_s^0 \to J/\psi\phi$ decay is among the most studied of the B_s^0-meson decays, owing to its relative abundance and high reconstruction efficiency. As such, this decay is used as the normalisation channel for several other B_s^0 decays [11–15]. Despite this, the precision on its branching fraction is still limited; the most precise measurement was performed by the LHCb experiment with pp collision data collected at $\sqrt{s} = 7\,\text{TeV}$, corresponding to an integrated luminosity of $1\,\text{fb}^{-1}$. This measurement yields $\mathcal{B}(B_s^0 \to J/\psi\phi) = (1.050 \pm 0.013 \pm 0.064 \pm 0.082) \times 10^{-3}$ [16], where the first uncertainty is statistical, the second systematic, including the external branching fraction measurement of $B^+ \to J/\psi K^+$ decays, and the third is due to the measurement of f_s/f_d [8]. Other measurements were performed by the Belle [17] and CDF [18] collaborations.

The $B_s^0 \to D_s^- \pi^+$ decay is another important B_s^0 meson decay mode, which is used as the normalisation channel for several hadronic B_s^0 decays with a single charm meson in the final state; its branching fraction can be used to test for the presence of physics beyond the SM in tree-level hadronic B decays [19]. However, the current precision on its branching fraction is also limited; the current best measurement by the LHCb experiment was performed using pp collision data collected at $\sqrt{s} = 7\,\text{TeV}$, corresponding to $0.37\,\text{fb}^{-1}$ of integrated luminosity. This measurement yields $\mathcal{B}(B_s^0 \to D_s^- \pi^+) = (2.95 \pm 0.05 \pm 0.17\,^{+0.18}_{-0.22}) \times 10^{-3}$ [20], where the first uncertainty is statistical, the second systematic, including the external branching fraction measurement of $B^0 \to D^- \pi^+$ decays, and the third due to the measurement of f_s/f_d taken from Ref. [8]. Other measurements were performed by the Belle [21] and CDF [22] collaborations.

The knowledge of B_s^0 branching fractions is thus often limited by the precision of the fragmentation fraction ratios. This paper presents a simultaneous determination of the fragmentation fractions and B_s^0 branching fractions with different decay modes. A combined analysis of LHCb measurements sensitive to f_s/f_d is performed, in order to

[1]The inclusion of the charge-conjugate modes is implied throughout this paper.

determine a precise value of this ratio as a function of $\sqrt{s}$ and p_{T} as well as the $B_s^0 \to J/\psi\phi$ and $B_s^0 \to D_s^-\pi^+$ branching fractions. This analysis employs previous LHCb measurements performed with ratios of semileptonic decays $B \to \overline{D}X\mu^+\nu_\mu$ at $\sqrt{s} = 7\,\mathrm{TeV}$ [8] and 13 TeV [23], where X denotes possible additional particles, hadronic $B \to Dh$ decays, where $h = \pi, K$, at $\sqrt{s} = 7$, 8 and 13 TeV [9,24], and $B \to J/\psi h'$ decays, where $h' = K, \phi$, at $\sqrt{s} = 7$, 8 and 13 TeV [10]. Measurements at 7 and 8 TeV were performed with data taken in 2010, 2011 and 2012, during Run 1 of the LHC; measurements at 13 TeV were performed with data taken in 2015 and 2016, during Run 2 of the LHC. Combinations of the Run 1 measurements were performed in Refs. [9,25] and are superseded by this paper.

The LHCb detector [26,27] is a single-arm forward spectrometer covering the pseudorapidity range $2 < \eta < 5$, designed for the study of particles containing b or c quarks. Simulation is used to model the effects of the detector acceptance and the imposed selection requirements. In the simulation, pp collisions are generated using PYTHIA [28] with a specific LHCb configuration [29]. Decays of unstable particles are described by EVTGEN [30], in which final-state radiation is generated using PHOTOS [31]. The interaction of the generated particles with the detector, and its response, are implemented using the GEANT4 toolkit [32] as described in Ref. [33].

The five sets of measurements that are combined in this paper rely on three different final states, referred to as semileptonic, hadronic, and charmonium final states. They are used to determine the ratio of efficiency-corrected yields, n_{corr}, of $B_s^0 \to Y$ decays relative to B^+ or $B^0 \to Z$ decays, which is sensitive to the ratio of branching fractions, $\mathcal{B}$, multiplied by $f_s/f_{d(u)}$,

$$\frac{n_{\mathrm{corr}}(B_s^0 \to Y)}{n_{\mathrm{corr}}(B^{0(+)} \to Z)} = \frac{\mathcal{B}(B_s^0 \to Y)}{\mathcal{B}(B^{0(+)} \to Z)} \frac{f_s}{f_{d(u)}} \quad , \tag{1}$$

where $\mathcal{B}$ is the exclusive branching fraction for the hadronic and charmonium measurements, and the inclusive one for the semileptonic measurement.

The various measurements have different ranges in pseudorapidity and transverse momentum of the B meson. The semileptonic and hadronic measurements are performed for $\eta \in [2, 5]$, while the charmonium measurement extends this range to $\eta \in [2, 6.4]$. As no pseudorapidity dependence is seen in the measurements under consideration, the fiducial region in which the combined analysis is considered valid includes the latter range. The combined analysis is performed as a function of p_{T} in the widest of the individual ranges, $p_{\mathrm{T}} \in [0.5, 40]\,\mathrm{GeV}/c$, which is used in the charmonium measurement; it is maintained as the fiducial region. The semileptonic measurement is performed for $p_{\mathrm{T}} \in [4, 25]\,\mathrm{GeV}/c$ and the hadronic measurement for $p_{\mathrm{T}} \in [1.5, 40]\,\mathrm{GeV}/c$.

The semileptonic measurements [8,23] use inclusive $B \to \overline{D}X\mu^+\nu_\mu$ decays, having reconstructed a ground state charm meson and a muon. The decay width of $b \to u$ decays is expected to be approximately 1% [7] of the total semileptonic width and almost equal for B_s^0, B^0 and B^+ mesons and is thus ignored. The modes studied are $B_s^0 \to D_s^- X\mu^+\nu_\mu$, $B_s^0 \to \overline{D}\overline{K}X\mu^+\nu_\mu$ for the B_s^0 meson and $B^{+,0} \to \overline{D}^0 X\mu^+\nu_\mu$ and $B^{+,0} \to D^- X\mu^+\nu_\mu$ for the B^+ and B^0 mesons, the contributions of which are not separated. As the $B_s^0 \to D^-\overline{K}^0 X\mu^+\nu_\mu$ final state cannot be reconstructed with high efficiency at the LHCb experiment, its contribution is inferred from the $B_s^0 \to \overline{D}^0 K^- X\mu^+\nu_\mu$ rate and the known decay modes of excited D_s^+ mesons to DK and D^*K final states. The charm mesons are reconstructed using the decays $D_s^- \to K^-K^+\pi^-$, $D^- \to K^+\pi^-\pi^-$ and $\overline{D}^0 \to K^+\pi^-$. The inclusive semileptonic decay widths for B_s^0, B^0 and B^+ mesons are almost equal, apart from an SU(3) breaking correction factor of $1-\xi_s = 1.010 \pm 0.005$ [34], and are normalised to the corresponding total widths through the ratio of B_s^0 over B^+ and B^0 lifetimes, denoted as $\tau_{B_s^0}$, τ_{B^+} and τ_{B^0}. Accordingly, $f_s/(f_u+f_d)$ is determined as

$$\begin{aligned}\frac{f_s}{f_u+f_d} =& \frac{n_{\text{corr}}(B_s^0\to D_s^- X\mu^+\nu_\mu) + n_{\text{corr}}(B_s^0\to \overline{D}\overline{K} X\mu^+\nu_\mu)}{n_{\text{corr}}(B^{+,0}\to \overline{D}{}^0 X\mu^+\nu_\mu) + n_{\text{corr}}(B^{+,0}\to D^- X\mu^+\nu_\mu)} \frac{\tau_{B^+}+\tau_{B^0}}{2\tau_{B_s^0}}(1-\xi_s) \\ &- \varepsilon_{\text{ratio}} \frac{\mathcal{B}(B^{+,0}\to D_s^- \overline{K} X\mu^+\nu_\mu)}{\mathcal{B}_{\text{SL}}} \quad , \end{aligned} \tag{2}$$

where the efficiency-corrected yields, n_{corr}, incorporate the relevant charm-meson branching fractions. The second term is small and is included to subtract the components from $B^{+,0}\to D_s^- \overline{K} X\mu^+\nu_\mu$ decays which are reconstructed in the $B_s^0\to D_s^- X\mu^+\nu_\mu$ sample, and contains $\varepsilon_{\text{ratio}}$, which is the ratio of efficiencies of reconstructing $B_s^0\to D_s^- X\mu^+\nu_\mu$ and $B^{+,0}\to D_s^- \overline{K} X\mu^+\nu_\mu$ through reconstruction of the $D_s^-\mu^+$ pair, and $\mathcal{B}_{\text{SL}}$, which is the semileptonic branching fraction of B_s^0 mesons [35]. The efficiency-corrected yields have been corrected for cross-feeds; *e.g.* those in the denominator have had cross-feed contributions, from $B_s^0, \Lambda_b^0 \to \overline{D} X\mu^+\nu_\mu$ decays, subtracted. The Run 1 measurement determines the integrated[2] value of $f_s/(f_u+f_d)$ at $\sqrt{s} = 7\,\text{TeV}$ using a data sample corresponding to an integrated luminosity of $3\,\text{pb}^{-1}$ [8]. The Run 2 measurement determines the value of $f_s/(f_u+f_d)$ in intervals of B-meson p_{T} at $\sqrt{s} = 13\,\text{TeV}$ using data corresponding to an integrated luminosity of $1.7\,\text{fb}^{-1}$ [23].

The hadronic measurements [9, 24] make use of $B^0\to D^-\pi^+$, $B^0\to D^-K^+$ and $B_s^0\to D_s^-\pi^+$ decays, using the same decay modes for the charm mesons as for the semileptonic analysis ($D_s^-\to K^-K^+\pi^-$ and $D^-\to K^+\pi^-\pi^-$). As the ratio of branching fractions of the $B_s^0\to D_s^-\pi^+$ decay relative to $B^0\to D^-h^+$ decays is predicted [36, 37], f_s/f_d can be determined according to

$$\frac{f_s}{f_d} = \Phi_{\text{PS},D^-K^+} \left|\frac{V_{us}}{V_{ud}}\right|^2 \left(\frac{f_K}{f_\pi}\right)^2 \frac{\tau_{B^0}}{\tau_{B_s^0}} \frac{1}{\mathcal{N}_a\mathcal{N}_F} \frac{\mathcal{B}(D^-\to K^+\pi^-\pi^-)}{\mathcal{B}(D_s^-\to K^-K^+\pi^-)} \frac{n_{\text{corr}}(B_s^0\to D_s^-\pi^+)}{n_{\text{corr}}(B^0\to D^-K^+)} \ , \tag{3a}$$

$$\frac{f_s}{f_d} = \Phi_{\text{PS},D^-\pi^+} \frac{\tau_{B^0}}{\tau_{B_s^0}} \frac{1}{\mathcal{N}_a\mathcal{N}_F\mathcal{N}_E} \frac{\mathcal{B}(D^-\to K^+\pi^-\pi^-)}{\mathcal{B}(D_s^-\to K^-K^+\pi^-)} \frac{n_{\text{corr}}(B_s^0\to D_s^-\pi^+)}{n_{\text{corr}}(B^0\to D^-\pi^+)} \quad , \tag{3b}$$

where Φ_{PS} is a phase-space factor, V_{us} and V_{ud} are the Cabibbo–Kobayashi–Maskawa (CKM) matrix elements, and f_K and f_π are the kaon and pion decay constants, which have permille uncertainties [7]. The remaining factors describe corrections to this ratio from non-factorisable effects, $\mathcal{N}_a$, the form factors, $\mathcal{N}_F$, and exchange diagram contributions to the $B^0\to D^-\pi^+$ decay, $\mathcal{N}_E$. The hadronic Run 1 measurement in Ref. [9] uses a data sample corresponding to an integrated luminosity of $1\,\text{fb}^{-1}$ at $\sqrt{s} = 7\,\text{TeV}$ and determines both ratios in Eq. (3a) and (3b). The integrated value of f_s/f_d is determined using Eq. (3a); the p_{T} dependence of f_s/f_d is determined in intervals of p_{T} using Eq. (3b). These results are included in a single dataset by scaling the p_{T} dependent measurement with the $D^-\pi^+$ final state to the integrated value of f_s/f_d measured with the D^-K^+ final state. The hadronic ratio measurement in Ref. [24] uses data samples corresponding to integrated luminosities of $1\,\text{fb}^{-1}$, $2\,\text{fb}^{-1}$ and $2\,\text{fb}^{-1}$ at $\sqrt{s} = 7$, 8 and 13 TeV, respectively, to

[2]Throughout this text, integrated f_s/f_d or $f_s/(f_u+f_d)$ refer to measurements integrated over B-meson kinematics.

determine the ratio with $D^-\pi^+$ final state in Eq. (3b), which is sensitive to the integrated value for f_s/f_d at each collision energy.

The charmonium measurement determines the p_{T} dependence of f_s/f_u at $\sqrt{s}=7$, 8 and 13 TeV using data samples corresponding to integrated luminosities of $1\,\mathrm{fb}^{-1}$, $2\,\mathrm{fb}^{-1}$ and $1.4\,\mathrm{fb}^{-1}$, respectively [10]. It uses the decay modes $B_s^0\to J/\psi\phi$ and $B^+\to J/\psi K^+$, where the ϕ meson decays to K^+K^-, and leads to

$$\frac{f_s}{f_u}=\frac{n_{\mathrm{corr}}(B_s^0\to J/\psi\phi)}{n_{\mathrm{corr}}(B^+\to J/\psi K^+)}\frac{\mathcal{B}(B^+\to J/\psi K^+)}{\mathcal{B}(B_s^0\to J/\psi\phi)\mathcal{B}(\phi\to K^+K^-)}=\frac{\mathcal{R}}{\mathcal{F}_R}\quad, \tag{4}$$

where $\mathcal{R}$ is the ratio of efficiency-corrected yields and $\mathcal{F}_R$ denotes the ratio of branching fractions. As no prediction is available for the ratio $\mathcal{F}_R$, this is included as a free parameter in the fit and is an additional result from this analysis.[3] The measurement in Ref. [16] includes a full amplitude analysis of the $B_s^0\to J/\psi K^+K^-$ decay in order to separate the components in the K^+K^- spectrum. The largest resonant contributions are from the $f_0(980)$, the ϕ, and the $f'(1525)$ mesons. In the mass region close to the ϕ resonance, in addition to the $f_0(980)$ meson, there is also a non-resonant S-wave component. The total S-wave fraction is in general not negligible [16] and varies as a function of the K^+K^- invariant mass. When considering a small window around the ϕ resonance mass, the S-wave contribution is significantly reduced. The $B_s^0\to J/\psi\phi$ measurement from Ref. [10], required a tight mass window of $\pm 10\,\mathrm{MeV}$ around the ϕ mass; therefore, the contribution of the S-wave component is suppressed to $(1.0\pm 0.2)\%$. This contribution is subtracted from the final value of the branching fraction reported in this paper.

To determine f_s/f_d, the semileptonic and hadronic measurements rely on external inputs from theory and experiment; most prominently, the D^-, $\overline{D}^0$ and D_s^- meson branching fractions to the considered decay modes, the B^+, B^0 and B_s^0 meson lifetimes, and the theory predictions for the $\mathcal{N}_a$, $\mathcal{N}_F$, and $\mathcal{N}_E$ parameters. In this combined analysis, all of the external inputs have been updated to their currently best known values, as shown in Table 1. For $\mathcal{B}(D_s^-\to K^-K^+\pi^-)$, a recent result from BESIII [40] is included and the weighted average of all current measurements is taken. For $\mathcal{N}_E$, the prediction from Ref. [37] is used, which is based on the ratio of branching fractions of the decays $B^0\to D^{*-}K^+$ and $B^0\to D^{*-}\pi^+$ and is updated using their current world averages [7]. The measurements and their uncertainties are thus rescaled to take into account the updated external inputs. The variation of the B-meson lifetimes could affect the estimates of the efficiencies used to determine f_s/f_d; it has been checked that this effect is negligible compared to the systematic uncertainties associated with each measurement.

The fit to the data is performed as a minimisation of the χ^2 function

$$\chi^2=(f(x|\theta)-y)V^{-1}(f(x|\theta)-y)^T+\sum_i\left(\frac{\theta_i-\hat{\theta}_i}{\sigma_{\theta_i}}\right)^2\quad, \tag{5}$$

where f is the function describing f_s/f_d in the data, with $x=p_{\mathrm{T}}$ or η, and y is the vector containing the central values of the measured observables sensitive to f_s/f_d, and V is their covariance matrix. The set of parameters to be determined, θ, includes a subset of

[3] In a measurement by the ATLAS collaboration [38] the ratio $\mathcal{R}$ was converted to a value for f_s/f_d using a prediction for the ratio of the $B_s^0\to J/\psi\phi$ and $B^0\to J/\psi K^{*0}$ branching fractions [39]. In this paper, results from Ref. [39] are not used because of disputed theoretical uncertainties arising from the assumption of factorisation.

Table 1: External inputs used in the hadronic and semileptonic analyses updated with respect to previous publications. The value of $\mathcal{N}_E$ is updated using Ref. [7]. The values of CKM matrix elements ratio $|V_{us}|/|V_{ud}|$ and of the meson decay constants' ratio f_K/f_π are the same as in Ref. [9].

Input	Value	Reference
$\mathcal{B}(\overline{D}^0 \to K^+\pi^-)$	$(3.999 \pm 0.045)\%$	[6]
$\mathcal{B}(D^- \to K^+\pi^-\pi^-)$	$(9.38 \pm 0.16)\%$	[7]
$\mathcal{B}(D_s^- \to K^-K^+\pi^-)$	$(5.47 \pm 0.10)\%$	[6,40]
$\tau_{B_s^0}/\tau_{B^0}$	1.006 ± 0.004	[6]
$(\tau_{B^+} + \tau_{B^0})/2\tau_{B_s^0}$	1.032 ± 0.005	[6]
$(1-\xi_s)$	1.010 ± 0.005	[34]
$\mathcal{N}_a$	1.000 ± 0.020	[37]
$\mathcal{N}_F$	1.000 ± 0.042	[19,41]
$\mathcal{N}_E$	0.966 ± 0.062	[7,37]
$\|V_{us}\|f_K/\|V_{ud}\|f_\pi$	0.2767	[9]

parameters that are constrained to external measurements $\hat{\theta}_i$ with their uncertainties σ_{θ_i}. While the first term in Eq. 5 is due to the experimental data compared with the function to be fitted, the second is due to external constraints on some of the parameters. These constraints are of two kinds: external constraints on theoretical input parameters and overall scaling parameters to take into account scale-related systematic uncertainties for some of the analyses. These uncertainties are not included in the data points, to avoid the bias described in Ref. [42], due to the failure of the intrinsic assumptions of the χ^2 method, and are thus taken into account as suggested in Ref. [43].

The scale factors related to the theoretical inputs, owing to their larger uncertainties, are found to have fitted values that differ from the input ones by up to one standard deviation. For this reason, these are kept indicated explicitly as ratios of the fitted value to the input value in the presentation of results. They are indicated by $r_{AF} = (\mathcal{N}_a\mathcal{N}_F)^{\text{fitted}}/(\mathcal{N}_a\mathcal{N}_F)^{\text{input}}$ for those common to the hadronic measurements and as $r_E = \mathcal{N}_E^{\text{fitted}}/\mathcal{N}_E^{\text{input}}$ for the exchange-diagram inputs.

The uncertainties from inputs common to the semileptonic and hadronic measurements, including the B-meson lifetimes and D-meson branching fractions, are 100% correlated among the hadronic measurements and 68% correlated with the semileptonic measurement, based on the relative rates of the $B_s^0 \to D_s^- X\mu^+\nu_\mu$ and $B_s^0 \to \overline{D}\overline{K}X\mu^+\nu_\mu$ decays and of the $B^{+,0} \to \overline{D}^0 X\mu^+\nu_\mu$ and $B^{+,0} \to D^- X\mu^+\nu_\mu$ decays.

The fit model as a function of p_{T} assumes the common functional form

$$\frac{f_s}{f_d}\,(p_{\mathrm{T}}, \sqrt{s}) = a + b \cdot p_{\mathrm{T}} \quad . \tag{6}$$

The dependence on collision energy is expressed by letting intercept a and slope b parameters have different values at different $\sqrt{s}$. Fits with different functional forms have been performed and the data can also be described with an exponential, Gaussian, or power-law functions, with similar fit quality. Attempts to describe the data with other functional forms suggested in Ref. [44] resulted in significantly worse fit quality. No attempt was made to describe the data with more parameters, with the exception of the

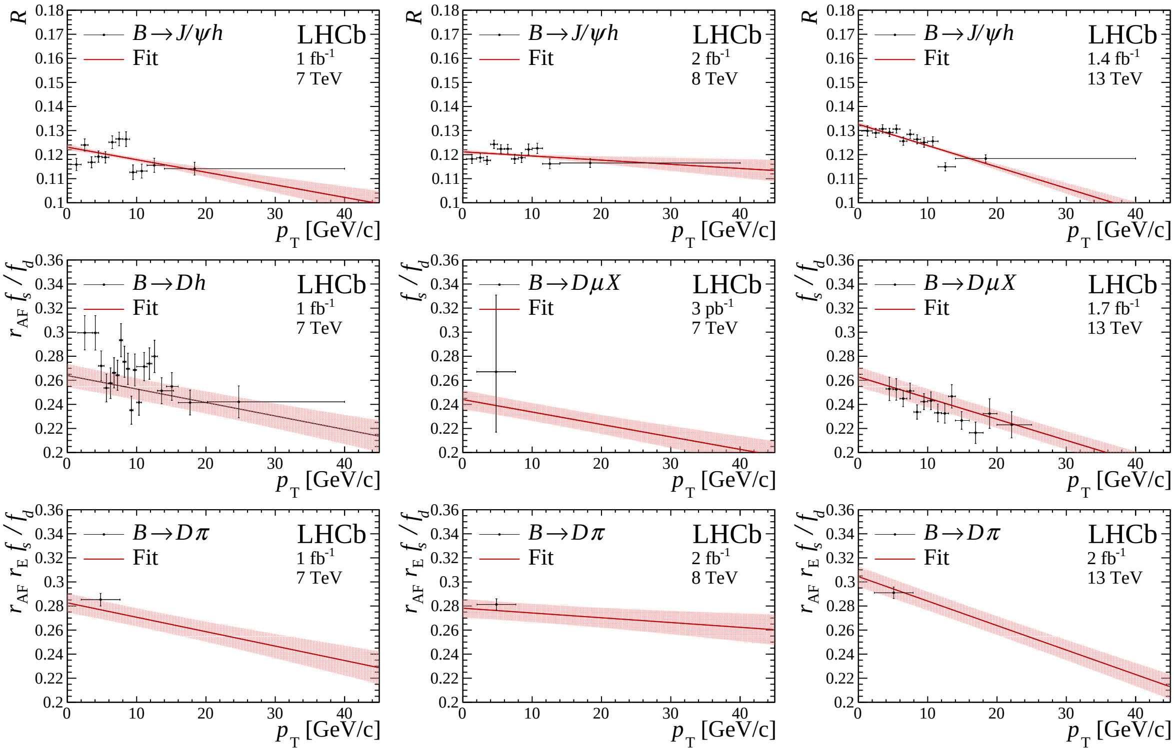

Figure 1: Measurements of f_s/f_d sensitive observables as a function of the B-meson transverse momentum, p_{T}, overlaid with the fit function. The scaling factors r_{AF} and r_E are defined in the text; the variable $\mathcal{R}$ is defined in Eq. 4. The vertical axes are zero-suppressed. The uncertainties on the data points are fully independent of each other; overall uncertainties for measurements in multiple p_{T} intervals are propagated via scaling parameters, as described in the text. The band associated with the fit function shows the uncertainty on the post-fit function for each sample.

physics-motivated fit with the Tsallis-statistics-inspired function, described at the end of the paper.

The data as a function of p_{T} together with the result of the fit are shown in Fig. 1. The obtained functions at the three different energies are

$$\begin{aligned}
f_s/f_d \quad (p_{\mathrm{T}}, 7\,\mathrm{TeV}) \quad &= (0.244 \pm 0.008) + ((-10.3 \pm 2.7) \times 10^{-4}) \cdot p_{\mathrm{T}} \ , \\
f_s/f_d \quad (p_{\mathrm{T}}, 8\,\mathrm{TeV}) \quad &= (0.240 \pm 0.008) + ((-\ \ 3.4 \pm 2.3) \times 10^{-4}) \cdot p_{\mathrm{T}} \ , \\
f_s/f_d \quad (p_{\mathrm{T}}, 13\,\mathrm{TeV}) \quad &= (0.263 \pm 0.008) + ((-17.6 \pm 2.1) \times 10^{-4}) \cdot p_{\mathrm{T}} \ ,
\end{aligned}$$

where the p_{T} is in units of GeV/c and the slope parameters are expressed in $(\mathrm{GeV}/c)^{-1}$. The resulting χ^2 is 133, for a number of effective degrees of freedom of 74. The statistical robustness of the procedure has been verified using ensembles of pseudoexperiments. They demonstrate that the procedure obtains the correct coverage and minimal bias for the parameters of interest. In the most extreme case, the bias corresponds to about 10% of the uncertainties on the parameters related to the overall scale. This is considered negligible and not corrected for. The p-value of the fit to data, calculated from the distribution of pseudoexperiment χ^2 values, is 1.4×10^{-4}. When artificially increasing the data uncertainties such that the χ^2 corresponds to a p-value of 0.5, following similar procedures to those in Ref. [7], the central values and uncertainties obtained in this paper are unchanged, with the exception of uncertainties on the slopes versus p_{T}, which would

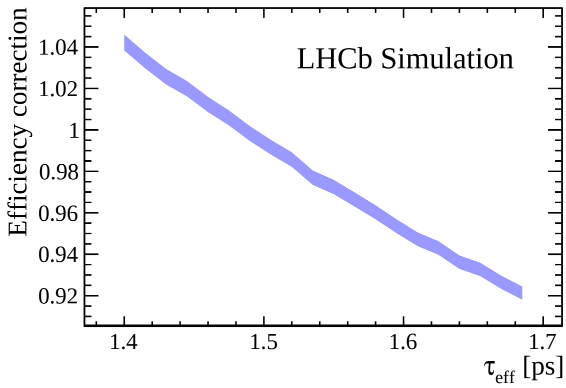

Figure 2: Efficiency correction versus effective lifetime hypothesis for the $B^0_s \to J/\psi\phi$ branching fraction. The band shows the uncertainty on the correction due to the simulated sample size for a given effective lifetime.

increase by approximately a relative 25% but not affect the integrated measurement of f_s/f_d. More data will be needed to resolve the exact p_{T} dependence of f_s/f_d.

Requiring identical intercepts and slopes at the three energies results in significantly worse fit quality, with a difference in χ^2 of 115 for two fewer parameters. An F-test [45] is performed to verify the significance of the dependence of the intercept on the energy; the difference in χ^2 corresponds to an F-test statistic of 13.2 and to a significance of 5.9 standard deviations (σ). Similarly, but less significantly, requiring only the slope parameters to be common among the energies increases the χ^2 by 22 for two fewer parameters, corresponding to an F-test significance of $2.7\,\sigma$.

Many of the input measurements also provide results as a function of pseudorapidity, none of them reporting any dependence on η. A combined fit as a function of η is also performed here. No dependence on pseudorapidity is found and the f_s/f_d value is found to be in agreement with the one obtained through the fit as a function of transverse momentum.

An additional output from the fit is $\mathcal{F}_R$, the ratio of the relative $B^0_s \to J/\psi\phi$ (with $\phi \to K^+K^-$) to $B^+ \to J/\psi K^+$ branching fractions, as in Eq. 4. The measurement of the $B^0_s \to J/\psi\phi$ branching fraction reported here is time-integrated, and as such should be compared with theoretical predictions that include a correction for the finite B^0_s-$\overline{B}^0_s$ width difference [46]. In addition, the total efficiency varies for different effective lifetimes; therefore, branching fraction measurements should be reported for a given effective lifetime value [47]. In this paper the results are obtained assuming the $B^0_s \to J/\psi\phi$ parameters measured in Ref. [48], which reports the time-dependent analysis of this decay, and the combination with previous LHCb measurements. The parameters used in this analysis correspond to a $B^0_s \to J/\psi\phi$ effective lifetime of $\tau_{\text{eff}} = 1.487\,\text{ps}$, which is different by 2.4% from that used in the simulation for the efficiency in Ref [10]. The $\mathcal{R}$ measurements are corrected to take this into account. A scaling for different effective lifetimes is reported in Fig. 2 and should be used as multiplicative correction to recompute the $B^0_s \to J/\psi\phi$ branching fraction under different hypotheses.

The fit value for the $\mathcal{F}_R$ parameter is 0.505 ± 0.016. The uncertainty is reduced to 0.012 when fixing external parameters, the remaining portion is dominated by the experimental systematic uncertainties on the input measurements. The $\mathcal{F}_R$ result can be converted to the $B_s^0 \to J/\psi\phi$ branching fraction including the $\phi \to K^+K^-$ decay branching fraction, by multiplying with the $B^+ \to J/\psi K^+$ branching fraction. The relative production fraction of B^+ and B^0 mesons at B Factories [49], 1.027 ± 0.037, is used to correct the input measurements [7] and the $B^+ \to J/\psi K^+$ branching fraction is found to be $(1.003 \pm 0.035) \times 10^{-3}$, resulting in

$$\mathcal{B}(B_s^0 \to J/\psi\phi, \phi \to K^+K^-) = (5.01 \pm 0.16 \pm 0.17) \times 10^{-4} \quad ,$$

where the first uncertainty includes statistical and systematic uncertainties on the yield ratio as well as the uncertainties on external parameters, and the second arises from the external measurement of $\mathcal{B}(B^+ \to J/\psi K^+)$. This result is corrected for the presence of the S-wave component and for the effective lifetime, as mentioned earlier. Taking into account the $\phi \to K^+K^-$ branching fraction, $(49.2 \pm 0.5)\%$ [7], the $B_s^0 \to J/\psi\phi$ branching fraction is

$$\mathcal{B}(B_s^0 \to J/\psi\phi) = (1.018 \pm 0.032 \pm 0.037) \times 10^{-3} \quad ,$$

where again the first uncertainty includes statistical and systematic uncertainties on the yield ratios as well as the uncertainties on external parameters, and the second is from external inputs. This result is compatible with and significantly more precise than the PDG world average of $(1.08 \pm 0.08) \times 10^{-3}$ [7]. It should be noted that the PDG average includes a measurement by the LHCb experiment at 7 TeV that is at least partially correlated with the 7 TeV data sample used in the $\mathcal{R}$ measurement included in this paper. The measurement is consistent with the individual measurements by the Belle collaboration, $(1.25 \pm 0.07 \pm 0.23) \times 10^{-3}$ [17], and the CDF collaboration, $(1.5 \pm 0.5 \pm 0.1) \times 10^{-3}$ [18], although these have larger uncertainties.

The ratio of the branching fractions of $B_s^0 \to D_s^-\pi^+$ and $B^0 \to D^-\pi^+$ decays is expressed in terms of the theory parameters in Eq. 3a. However, the theory constraints can be removed and the fit can be repeated to estimate this quantity from data. The normalisation of the f_s/f_d function is correspondingly shifted by a relative 2.5%, which is within the final uncertainties. The other parameters are found to be in good agreement. The uncertainties on all parameters do not change significantly with respect to the default fit. The output of this fit is then converted to a measurement of the abovementioned ratio of branching fractions. The result is

$$\frac{\mathcal{B}(B_s^0 \to D_s^-\pi^+)}{\mathcal{B}(B^0 \to D^-\pi^+)} = 1.18 \pm 0.04 \quad ,$$

where the correlation of the D-meson branching fractions is considered when calculating this uncertainty. The uncertainty is reduced to 0.033 when fixing external parameters; the remaining portion is dominated by the experimental systematic uncertainties on the input measurements. This result can be compared with the ratio measured by the LHCb collaboration using only 2011 data [20], which yields $\mathcal{B}(B_s^0 \to D_s^-\pi^+)/\mathcal{B}(B^0 \to D^-\pi^+) = 1.10 \pm 0.018 \pm 0.033\,^{+0.07}_{-0.08}$, where the uncertainties are statistical, systematic and due to f_s/f_d, and with the current ratio of PDG averages of 1.19 ± 0.19 [7]. This result is in excellent agreement with both and significantly more precise. The relative production fraction of B^+ and B^0 mesons at the B Factories [49], 1.027 ± 0.037, is used to correct the input measurements for the $B^0 \to D^-\pi^+$ branching fraction [7]; it is found to be

$(2.72 \pm 0.14) \times 10^{-3}$. Using this value, the branching fraction of $B_s^0 \to D_s^- \pi^+$ decays is measured to be

$$\mathcal{B}(B_s^0 \to D_s^- \pi^+) = (3.20 \pm 0.10 \pm 0.16) \times 10^{-3} \quad ,$$

where the first uncertainty is due to the total experimental uncertainties on the yield ratios and the uncertainties from external parameters and the second is due to the $B^0 \to D^- \pi^+$ branching fraction. This result is in agreement with and significantly more precise than the previous LHCb measurement [20], $\mathcal{B}(B_s^0 \to D_s^- \pi^+) = (2.95 \pm 0.05 \pm 0.17^{+0.18}_{-0.22}) \times 10^{-3}$, where the uncertainties are again statistical, systematic and due to f_s/f_d, and the PDG average, $(3.00 \pm 0.23) \times 10^{-3}$, which is dominated by the latter.

Reference p_{T} spectra, needed to calculate the integrated f_s/f_d ratios, are obtained by generating B_s^0 and B^0 mesons in the fiducial acceptance, without any simulation of the detector. The average p_{T} for these spectra are very similar for B_s^0 and B^0 mesons; they are is 4.80, 4.85 and 5.10 GeV/c for the $\sqrt{s} = 7$, 8 and 13 TeV generated samples, respectively, with a standard deviation of about 2.8 GeV/c at all energies. The following integrated f_s/f_d values for $p_{\mathrm{T}} \in [0.5, 40]$ GeV/c and $\eta \in [2, 6.4]$ are measured

$$\begin{aligned} f_s/f_d\,(7\,\mathrm{TeV}) &= 0.2390 \pm 0.0076 \quad , \\ f_s/f_d\,(8\,\mathrm{TeV}) &= 0.2385 \pm 0.0075 \quad , \\ f_s/f_d\,(13\,\mathrm{TeV}) &= 0.2539 \pm 0.0079 \quad , \end{aligned}$$

which are shown in Fig. 3. Ratios of the integrated values at different energies have also been calculated, incorporating correlations between the uncertainties, yielding

$$\begin{aligned} \frac{f_s/f_d\,(13\,\mathrm{TeV})}{f_s/f_d\,(7\,\mathrm{TeV})} &= 1.064 \pm 0.008 \quad , \\ \frac{f_s/f_d\,(13\,\mathrm{TeV})}{f_s/f_d\,(8\,\mathrm{TeV})} &= 1.065 \pm 0.007 \quad , \\ \frac{f_s/f_d\,(8\,\mathrm{TeV})}{f_s/f_d\,(7\,\mathrm{TeV})} &= 0.998 \pm 0.008 \quad , \end{aligned}$$

which can be used to correctly normalise future analyses using data at different energies. These values are calculated assuming an equal average p_{T} of 5 GeV/c for the different energies, however, it has been verified that varying this assumption does not modify the results significantly. In addition, the ratio of the Run 2 (13 TeV) over Run 1 (7 and 8 TeV) measurements has been computed, weighting the Run 1 values by their integrated luminosity (1 and 2 fb^{-1}, respectively), resulting in

$$\frac{f_s/f_d\,(\mathrm{Run\ 2})}{f_s/f_d\,(\mathrm{Run\ 1})} = 1.064 \pm 0.007 \quad .$$

Using the results for the integrated f_s/f_d, $\mathcal{B}(B_s^0 \to J/\psi\phi)$ and $\mathcal{B}(B_s^0 \to D_s^- \pi^+)$, previous LHCb measurements of B_s^0 branching fractions are updated by scaling these with either f_s/f_d and a B^0 or B^+ branching fraction, or with the associated normalisation B_s^0 branching fraction. The B^0 and B^+ normalisation branching fractions are updated using the current PDG world averages [7], corrected for the relative production fraction of B^+ and B^0 mesons at the B Factories [49]. The sole exception is $\mathcal{B}(B^0 \to J/\psi K^{*0})$, for

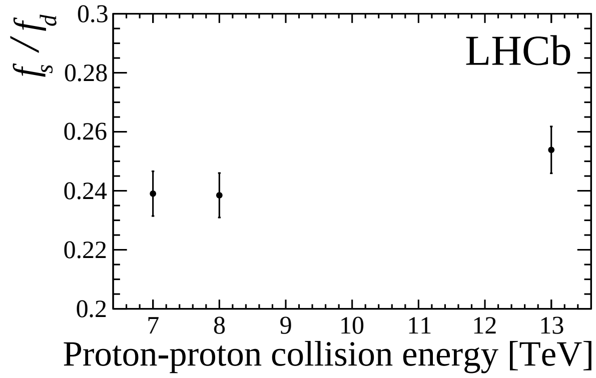

Figure 3: Fragmentation fraction ratio f_s/f_d as a function of proton-proton centre-of-mass energy.

which the branching fraction is taken from the result of the only amplitude analysis, as performed by the Belle experiment [50]. The B^0 and B^+ normalisation branching fractions are presented in Table 2. For LHCb measurements using both Run 1 and Run 2 data, an average f_s/f_d is estimated using the relative expected yields at the different energies, with the uncertainties from f_s/f_d and normalisation mode branching fractions recomputed accordingly. Updating these inputs significantly reduces the systematic uncertainty from f_s/f_d on all previous B^0_s branching fraction measurements, such that the updated results supersede those from the cited publications. The only exception is the branching fraction of $B^0_s \to \mu^+\mu^-$ decays, for which the LHCb result updated here has less precision than the LHC-wide average determined recently [51], and which will be superseded only by future updates of this measurement with the full Run 2 data sample. The updated branching fractions are grouped according to decay type: rare B^0_s decays are updated in Table 3, B^0_s decays with charmonium in Table 4, charmless B^0_s decays in Table 5, and B^0_s decays with charm mesons in Table 6. As the estimated value of f_s/f_d for the Run 1 data samples decreased, in general the values of the branching fractions increase with respect to their published values; the branching fractions normalised to $B^0_s \to J/\psi\phi$ and $B^0_s \to D^-_s\pi^+$ instead decrease with respect to their published values.

The recent measurement of $|V_{cb}|$ with $B^0_s \to D^{(*)-}_s\mu^+\nu_\mu$ decays using Run 1 data [52], also relies on an estimate of f_s/f_d and is independent of the uncertainty on the product $\mathcal{B}(D^-_s \to K^-K^+\pi^-) \times \tau_{B^0_s}$. For this estimate, the correlation of f_s/f_d with $\mathcal{B}(D^-_s \to K^-K^+\pi^-)$ from the semileptonic measurement is used. The resulting estimates for $|V_{cb}|$ are $|V_{cb}|_{\mathrm{CLN}} = (40.8 \pm 0.6 \pm 0.9 \pm 1.1) \times 10^{-3}$, $|V_{cb}|_{\mathrm{BGL}} = (41.7 \pm 0.8 \pm 0.9 \pm 1.1) \times 10^{-3}$, where CLN [53] and BGL [54] stand for two hadronic form-factor parametrisations. Both results are consistent with the current world average (see for example Ref. [7]).

The p_{T} distribution of produced mesons is often described through a function inspired by the Tsallis statistics [93, 94]. Examples of this use can be found in Refs. [95–99]. In particular, factoring out the pseudorapidity-dependent part, this function is often written as

$$\frac{dN}{dp_{\mathrm{T}}} = C\frac{(n-1)(n-2)}{nT(nT+Mc^2(n-2))}p_{\mathrm{T}}\left[1+\frac{\sqrt{M^2c^4+p_T^2c^2}-Mc^2}{nT}\right]^{-n} \quad , \tag{7}$$

Table 2: The branching fractions of B^0 and B^+ normalisation channel decays used to update previous measurements of B_s^0 branching fractions, as reported in Ref. [7] for all but the $B^0 \to J/\psi K^{*0}$ branching fraction, which is taken from the amplitude analysis in Ref [50], and corrected for the relative production fraction of B^+ and B^0 mesons at B Factories [49].

Decay mode	Branching fraction	Decay mode	Branching fraction
$B^0 \to J/\psi K^{*0}$	$(1.21 \pm 0.08) \times 10^{-3}$	$B^0 \to D^- \mu^+ \nu_\mu$	$(2.31 \pm 0.10)\%$
$B^0 \to J/\psi \rho^0$	$(2.58 \pm 0.18) \times 10^{-5}$	$B^0 \to D^{*-} \mu^+ \nu_\mu$	$(5.05 \pm 0.14)\%$
$B^0 \to J/\psi K_S^0$	$(4.40 \pm 0.17) \times 10^{-3}$	$B^0 \to D^{*\pm} D^{\mp}$	$(6.2 \pm 0.6) \times 10^{-4}$
$B^0 \to J/\psi K_S^0 \pi^+ \pi^-$	$(2.18 \pm 0.19) \times 10^{-3}$	$B^0 \to D^+ D^-$	$(2.14 \pm 0.19) \times 10^{-4}$
$B^0 \to \psi(2S) K^{*0}$	$(5.98 \pm 0.42) \times 10^{-4}$	$B^0 \to D^- D_s^+$	$(7.3 \pm 0.8) \times 10^{-3}$
$B^0 \to \psi(2S) K^+ \pi^-$	$(5.88 \pm 0.42) \times 10^{-4}$	$B^+ \to \overline{D}^0 D_s^+$	$(9.0 \pm 0.9) \times 10^{-3}$
$B^0 \to K^+ \pi^-$	$(1.98 \pm 0.07) \times 10^{-5}$	$B^0 \to \overline{D}^0 \pi^+ \pi^-$	$(8.8 \pm 0.5) \times 10^{-4}$
$B^0 \to K_S^0 \pi^+ \pi^-$	$(2.51 \pm 0.11) \times 10^{-5}$	$B^0 \to \overline{D}^0 \rho$	$(3.21 \pm 0.21) \times 10^{-4}$
$B^0 \to K^{*+} \pi^-$	$(7.60 \pm 0.43) \times 10^{-6}$	$B^0 \to \overline{D}^0 K_S^0$	$(5.3 \pm 0.7) \times 10^{-5}$
$B^0 \to p\overline{p} K^+ \pi^-$	$(6.30 \pm 0.50) \times 10^{-6}$	$B^0 \to \overline{D}^0 K^+ K^-$	$(6.1 \pm 0.6) \times 10^{-5}$
$B^0 \to p \overline{\Lambda} \pi^-$	$(3.18 \pm 0.30) \times 10^{-6}$		
$B^0 \to K^{*0} \gamma$	$(4.13 \pm 0.26) \times 10^{-5}$		
$B^0 \to \phi K_S^0$	$(3.70 \pm 0.36) \times 10^{-6}$		
$B^0 \to \phi K^{*0}$	$(1.01 \pm 0.05) \times 10^{-5}$		

where M is the mass of the meson, n and T are parameters linked to the Tsallis statistics, and C is a normalisation constant. An attempt has been made to describe the data with a ratio of two such Tsallis functions. Reasonable agreement, albeit with large fit instabilities due to parametrisation ambiguities, is obtained when considering the same value for the T parameter for the B_s^0 and B^0 mesons, and with the n differing by a factor of 0.9 between B_s^0 and B^0 mesons. The results of this fit tantalisingly reproduce the stabilisation, or even decrease, of the f_s/f_d seen in the data at low p_T values, and are reported in Fig. 4. The branching fractions obtained with this parametrisation are in agreement with the default fit, but have larger uncertainties due to the fit instability.

In conclusion, this paper presents a precise measurement of the ratio of B_s^0 and B^0 fragmentation fractions, f_s/f_d, as a function of pp centre-of-mass energy $\sqrt{s}$ and B-meson p_T, from the combined analysis of LHCb measurements. A significant dependence of f_s/f_d on $\sqrt{s}$ and p_T, described by linear functions, is observed. Precise measurements of the $B_s^0 \to J/\psi \phi$ and $B_s^0 \to D_s^- \pi^+$ branching fractions are also obtained, halving their uncertainties with respect to previous world averages. Finally, previous LHCb measurements of B_s^0 branching fractions are updated, strongly reducing their normalisation-related uncertainties and better constraining possible contributions from physics beyond the SM.

Table 3: Updated branching fractions of rare B_s^0 decays. The uncertainties are statistical, systematic, due to f_s/f_d, and due to the normalisation branching fraction. The $B_s^0 \to \phi\mu^+\mu^-$ branching fractions in different q^2 intervals, where q^2 is defined as dimuon invariant mass squared in GeV/c^2, are normalised with respect to $B_s^0 \to J/\psi\phi$. Results with the $\star$ symbol have had their normalisation branching fraction updated as well.

Decay mode	Updated branching fraction	Previous result		
$B_s^0 \to \phi\gamma$	$(3.75 \pm 0.18 \pm 0.12 \pm 0.12 \pm 0.24) \times 10^{-5}$	$(3.52 \pm 0.17 \pm 0.11 \pm 0.29 \pm 0.12) \times 10^{-5}$	[55]	$\star$
$B_s^0 \to \mu^+\mu^-$	$(3.26 \pm 0.65^{+0.22}_{-0.11} \pm 0.10) \times 10^{-9}$	$(3.0 \pm 0.6^{+0.2}_{-0.1} \pm 0.2) \times 10^{-9}$	[56]	
$B_s^0 \to \overline{K}^{*0}\mu^+\mu^-$	$(3.09 \pm 1.07 \pm 0.21 \pm 0.10 \pm 0.22) \times 10^{-8}$	$(2.9 \pm 1.0 \pm 0.2 \pm 0.2 \pm 0.2) \times 10^{-8}$	[57]	
$B_s^0 \to \pi^+\pi^-\mu^+\mu^-$	$(8.66 \pm 1.50 \pm 0.47 \pm 0.28 \pm 0.60) \times 10^{-8}$	$(8.6 \pm 1.5 \pm 0.5 \pm 0.5 \pm 0.7) \times 10^{-8}$	[58]	$\star$
$B_s^0 \to \phi\mu^+\mu^-$	$(7.54^{+0.43}_{-0.41} \pm 0.30 \pm 0.36) \times 10^{-7}$	$(7.97^{+0.45}_{-0.43} \pm 0.32 \pm 0.60) \times 10^{-7}$	[14]	$\star$
$q^2 \in [1.0, 6.0]$	$(2.44^{+0.31}_{-0.30} \pm 0.07 \pm 0.12) \times 10^{-8}$	$(2.58^{+0.33}_{-0.31} \pm 0.08 \pm 0.19) \times 10^{-8}$	[14]	$\star$
$q^2 \in [15.0, 19.0]$	$(3.82^{+0.38}_{-0.36} \pm 0.12 \pm 0.18) \times 10^{-8}$	$(4.04^{+0.39}_{-0.38} \pm 0.13 \pm 0.30) \times 10^{-8}$	[14]	$\star$
$q^2 \in [0.1, 2.0]$	$(5.54^{+0.69}_{-0.65} \pm 0.13 \pm 0.27) \times 10^{-8}$	$(5.85^{+0.73}_{-0.69} \pm 0.14 \pm 0.44) \times 10^{-8}$	[14]	$\star$
$q^2 \in [2.0, 5.0]$	$(2.42^{+0.40}_{-0.38} \pm 0.06 \pm 0.12) \times 10^{-8}$	$(2.56^{+0.42}_{-0.39} \pm 0.06 \pm 0.19) \times 10^{-8}$	[14]	$\star$
$q^2 \in [5.0, 8.0]$	$(3.03^{+0.42}_{-0.40} \pm 0.07 \pm 0.15) \times 10^{-8}$	$(3.21^{+0.44}_{-0.42} \pm 0.08 \pm 0.24) \times 10^{-8}$	[14]	$\star$
$q^2 \in [11.0, 12.5]$	$(4.45^{+0.65}_{-0.62} \pm 0.14 \pm 0.21) \times 10^{-8}$	$(4.71^{+0.69}_{-0.65} \pm 0.15 \pm 0.36) \times 10^{-8}$	[14]	$\star$
$q^2 \in [15.0, 17.0]$	$(4.28^{+0.54}_{-0.51} \pm 0.11 \pm 0.21) \times 10^{-8}$	$(4.52^{+0.57}_{-0.54} \pm 0.12 \pm 0.34) \times 10^{-8}$	[14]	$\star$
$q^2 \in [17.0, 19.0]$	$(3.75^{+0.54}_{-0.51} \pm 0.13 \pm 0.18) \times 10^{-8}$	$(3.96^{+0.57}_{-0.54} \pm 0.14 \pm 0.30) \times 10^{-8}$	[14]	$\star$

Table 4: Updated branching fractions of B_s^0 decays with charmonia in the final state. The uncertainties are statistical, systematic, due to f_s/f_d, and due to the normalisation branching fraction. The second, third and fourth set of branching fractions are normalised to $B_s^0 \to J/\psi\phi$, $B_s^0 \to J/\psi\eta^{(\prime)}$, $B_s^0 \to J/\psi\pi^+\pi^-$, respectively, and their third uncertainty covers the full normalisation uncertainty. Results with the $\star$ symbol have had their normalisation branching fraction updated as well.

Decay mode	Updated branching fraction	Previous result		
$B_s^0 \to J/\psi K^0_S$	$(2.06 \pm 0.08 \pm 0.06 \pm 0.07 \pm 0.08) \times 10^{-5}$	$(1.93 \pm 0.08 \pm 0.05 \pm 0.11 \pm 0.07) \times 10^{-5}$	[59]	
$B_s^0 \to J/\psi K^0_S K^\pm\pi^\mp$	$(5.01 \pm 0.35 \pm 0.33 \pm 0.16 \pm 0.44) \times 10^{-4}$	$(4.6 \pm 0.3 \pm 0.3 \pm 0.3 \pm 0.4) \times 10^{-4}$	[60]	$\star$
$B_s^0 \to \psi(2S)\overline{K}^{*0}$	$(3.62 \pm 0.37 \pm 0.26 \pm 0.12 \pm 0.25) \times 10^{-5}$	$(3.35 \pm 0.34 \pm 0.24 \pm 0.19 \pm 0.22) \times 10^{-5}$	[61]	
$B_s^0 \to \psi(2S)K^+\pi^-$	$(3.43 \pm 0.23 \pm 0.14 \pm 0.11 \pm 0.24) \times 10^{-5}$	$(3.12 \pm 0.21 \pm 0.13 \pm 0.18 \pm 0.22) \times 10^{-5}$	[61]	
$B_s^0 \to J/\psi\eta$	$(4.04 \pm 0.35^{+0.32}_{-0.43} \pm 0.13 \pm 0.28) \times 10^{-4}$	$(3.79 \pm 0.31^{+0.20}_{-0.41} \pm 0.28 \pm 0.56) \times 10^{-4}$	[62]	$\star$
$B_s^0 \to J/\psi\eta'$	$(3.67 \pm 0.32^{+0.14}_{-0.38} \pm 0.12 \pm 0.25) \times 10^{-4}$	$(3.42 \pm 0.30^{+0.14}_{-0.35} \pm 0.26 \pm 0.51) \times 10^{-4}$	[62]	$\star$
$B_s^0 \to \psi(2S)\phi$	$(4.98 \pm 0.26 \pm 0.24 \pm 0.24) \times 10^{-4}$	$(5.33 \pm 0.28 \pm 0.26^{+1.37}_{-1.12}) \times 10^{-4}$	[12]	$\star$
$B_s^0 \to \chi_{c1}\phi$	$(1.92 \pm 0.18 \pm 0.14 \pm 0.09) \times 10^{-5}$	$(1.98 \pm 0.19 \pm 0.15 \pm 0.20) \times 10^{-5}$	[63]	$\star$
$B_s^0 \to J/\psi\pi^+\pi^-$	$(2.01 \pm 0.05 \pm 0.05 \pm 0.10) \times 10^{-4}$	$(2.16 \pm 0.05 \pm 0.06^{+0.51}_{-0.42}) \times 10^{-4}$	[11]	$\star$
$B_s^0 \to J/\psi\phi\phi$	$(1.17 \pm 0.12^{+0.05}_{-0.09} \pm 0.06) \times 10^{-5}$	$(1.19 \pm 0.12^{+0.05}_{-0.09} \pm 0.10) \times 10^{-5}$	[15]	$\star$
$B_s^0 \to J/\psi\overline{K}^{*0}$	$(4.12 \pm 0.19 \pm 0.13 \pm 0.20) \times 10^{-5}$	$(4.20 \pm 0.20 \pm 0.13 \pm 0.36) \times 10^{-5}$	[64]	$\star$
$B_s^0 \to J/\psi p\bar{p}$	$(3.54 \pm 0.19 \pm 0.24 \pm 0.16) \times 10^{-6}$	$(3.58 \pm 0.19 \pm 0.24 \pm 0.30) \times 10^{-6}$	[65]	$\star$
$B^0 \to J/\psi p\bar{p}$	$(3.94 \pm 0.35 \pm 0.26 \pm 0.13) \times 10^{-7}$	$(4.51 \pm 0.40 \pm 0.30 \pm 0.32) \times 10^{-7}$	[65]	$\star$
$B_s^0 \to \psi(2S)\eta$	$(3.35 \pm 0.57 \pm 0.48 \pm 0.50) \times 10^{-4}$	$(3.15 \pm 0.53 \pm 0.45^{+0.61}_{-0.67}) \times 10^{-4}$	[66]	$\star$
$B_s^0 \to \psi(2S)\eta'$	$(1.42 \pm 0.33 \pm 0.06 \pm 0.20) \times 10^{-4}$	$(1.32 \pm 0.31 \pm 0.05^{+0.26}_{-0.28}) \times 10^{-4}$	[67]	$\star$
$B_s^0 \to J/\psi\pi^+\pi^-\pi^+\pi^-$	$(7.49 \pm 0.30 \pm 0.44 \pm 0.42) \times 10^{-5}$	$(7.62 \pm 0.36 \pm 0.64 \pm 0.42) \times 10^{-5}$	[68]	$\star$
$B_s^0 \to \psi(2S)\pi^+\pi^-$	$(6.87 \pm 0.81 \pm 0.65 \pm 0.39) \times 10^{-5}$	$(7.3 \pm 0.9 \pm 0.6^{+1.9}_{-1.6}) \times 10^{-5}$	[66]	$\star$

Table 5: Updated branching fractions of B_s^0 decays with a charmless final state. The uncertainties are statistical, systematic, due to f_s/f_d, and due to the normalisation branching fraction. The last two branching fractions are normalised with respect to $B_s^0 \to \phi\phi$, and their third uncertainty covers the full normalisation uncertainty. Results with the $\star$ symbol have had their normalisation branching fraction updated as well.

Decay mode	Updated branching fraction	Previous result		
$B_s^0 \to \pi^+\pi^-$	$(7.60 \pm 0.58 \pm 0.69 \pm 0.25 \pm 0.25) \times 10^{-7}$	$(6.91 \pm 0.54 \pm 0.63 \pm 0.40 \pm 0.19) \times 10^{-7}$	[69]	
$B_s^0 \to K^-\pi^+$	$(6.15 \pm 0.49 \pm 0.49 \pm 0.20 \pm 0.20) \times 10^{-6}$	$(5.4 \pm 0.4 \pm 0.4 \pm 0.4 \pm 0.2) \times 10^{-6}$	[70]	$\star$
$B_s^0 \to K^+K^-$	$(2.63 \pm 0.08 \pm 0.16 \pm 0.09 \pm 0.09) \times 10^{-5}$	$(2.30 \pm 0.07 \pm 0.14 \pm 0.17 \pm 0.07) \times 10^{-5}$	[70]	$\star$
$B_s^0 \to K_S^0 K_S^0$	$(8.28 \pm 1.60 \pm 0.90 \pm 0.26 \pm 0.81) \times 10^{-6}$	$(8.3 \pm 1.6 \pm 0.9 \pm 0.3 \pm 0.8) \times 10^{-6}$	[71]	
$B_s^0 \to K_S^0 \pi^+\pi^-$	$(5.21 \pm 0.74 \pm 0.85 \pm 0.17 \pm 0.23) \times 10^{-6}$	$(4.7 \pm 0.7 \pm 0.8 \pm 0.3 \pm 0.2) \times 10^{-6}$	[72]	
$B_s^0 \to K_S^0 K^\pm\pi^\mp$	$(4.64 \pm 0.19 \pm 0.30 \pm 0.15 \pm 0.21) \times 10^{-5}$	$(4.22 \pm 0.18 \pm 0.28 \pm 0.25 \pm 0.17) \times 10^{-5}$	[72]	
$B_s^0 \to K^{*0}\overline{K}^{*0}$	$(2.70 \pm 0.44 \pm 0.43 \pm 0.09 \pm 0.19) \times 10^{-5}$	$(2.81 \pm 0.46 \pm 0.43 \pm 0.34 \pm 0.13) \times 10^{-5}$	[73]	$\star$
$B_s^0 \to K^{*\pm}K^\mp$	$(1.23 \pm 0.18 \pm 0.13 \pm 0.04 \pm 0.07) \times 10^{-5}$	$(1.27 \pm 0.19 \pm 0.13 \pm 0.07 \pm 0.10) \times 10^{-5}$	[74]	
$B_s^0 \to K^{*-}\pi^+$	$(3.21 \pm 1.07 \pm 0.41 \pm 0.10 \pm 0.18) \times 10^{-6}$	$(3.3 \pm 1.1 \pm 0.4 \pm 0.2 \pm 0.3) \times 10^{-6}$	[74]	
$B_s^0 \to p\bar{p}K^\pm\pi^\mp$	$(1.41 \pm 0.23 \pm 0.12 \pm 0.05 \pm 0.11) \times 10^{-6}$	$(1.30 \pm 0.21 \pm 0.11 \pm 0.09 \pm 0.08) \times 10^{-6}$	[75]	
$B_s^0 \to \overset{(-)}{p}\overset{(-)}{\Lambda}K^\mp$	$(6.01 \pm 0.66 \pm 0.62 \pm 0.20 \pm 0.57) \times 10^{-6}$	$(5.46 \pm 0.61 \pm 0.57 \pm 0.32 \pm 0.50) \times 10^{-6}$	[76]	
$B_s^0 \to \phi\overline{K}^{*0}$	$(1.27 \pm 0.28 \pm 0.16 \pm 0.04 \pm 0.07) \times 10^{-6}$	$(1.10 \pm 0.24 \pm 0.13 \pm 0.08 \pm 0.06) \times 10^{-6}$	[77]	$\star$
$B_s^0 \to \phi\phi$	$(2.02 \pm 0.05 \pm 0.08 \pm 0.07 \pm 0.11) \times 10^{-5}$	$(1.84 \pm 0.05 \pm 0.07 \pm 0.11 \pm 0.12) \times 10^{-5}$	[78]	
$B_s^0 \to \phi\pi^+\pi^-$	$(3.82 \pm 0.25 \pm 0.19 \pm 0.30) \times 10^{-6}$	$(3.48 \pm 0.23 \pm 0.17 \pm 0.35) \times 10^{-6}$	[79]	$\star$
$B_s^0 \to \phi\phi\phi$	$(2.36 \pm 0.61 \pm 0.30 \pm 0.19) \times 10^{-6}$	$(2.15 \pm 0.54 \pm 0.28 \pm 0.21) \times 10^{-6}$	[80]	$\star$

Table 6: Updated branching fractions of B_s^0 decays to open-charm final states. The uncertainties are statistical, systematic, due to f_s/f_d, and due to the normalisation branching fraction. The $B_s^0 \to D_s^{\mp}K^{\pm}$, $B_s^0 \to D_s^-\pi^+\pi^-\pi^+$ and $B_s^0 \to D_s^-K^+\pi^-\pi^+, B_s^0 \to D_{s1}(2536)^-\pi^+$ branching fractions are normalised with respect to $B_s^0 \to D_s^-\pi^+$ and $B_s^0 \to D_s^-\pi^+\pi^-\pi^+$, respectively, and their third uncertainty covers the full normalisation uncertainty. Results with the $\star$ symbol have had their normalisation branching fraction updated as well.

Decay mode	Updated branching fraction	Previous result		
$B_s^0 \to D_s^{*-}\mu^+\nu_\mu$	$(5.19 \pm 0.24 \pm 0.47 \pm 0.13 \pm 0.14) \times 10^{-2}$	$(5.38 \pm 0.25 \pm 0.48 \pm 0.20 \pm 0.15) \times 10^{-2}$	[52]	
$B_s^0 \to D_s^-\mu^+\nu_\mu$	$(2.40 \pm 0.12 \pm 0.15 \pm 0.06 \pm 0.10) \times 10^{-2}$	$(2.49 \pm 0.12 \pm 0.16 \pm 0.09 \pm 0.11) \times 10^{-2}$	[52]	
$B_s^0 \to D^+D_s^-$	$(3.01 \pm 0.32 \pm 0.10 \pm 0.08 \pm 0.34) \times 10^{-4}$	$(2.7 \pm 0.3 \pm 0.1 \pm 0.2 \pm 0.3) \times 10^{-4}$	[81]	
$B_s^0 \to D^+D^-$	$(2.47 \pm 0.46 \pm 0.23 \pm 0.08 \pm 0.22) \times 10^{-4}$	$(2.2 \pm 0.4 \pm 0.1 \pm 0.1 \pm 0.3) \times 10^{-4}$	[82]	
$B_s^0 \to D^0\overline{D}^0$	$(1.83 \pm 0.29 \pm 0.29 \pm 0.05 \pm 0.18) \times 10^{-4}$	$(1.9 \pm 0.3 \pm 0.2 \pm 0.2 \pm 0.3) \times 10^{-4}$	[82]	
$B_s^0 \to D_s^+D_s^-$	$(4.38 \pm 0.23 \pm 0.31 \pm 0.11 \pm 0.49) \times 10^{-3}$	$(4.0 \pm 0.2 \pm 0.2 \pm 0.2 \pm 0.4) \times 10^{-3}$	[82]	
$B_s^0 \to D^{*\pm}D^{*\mp}$	$(8.38 \pm 1.02 \pm 0.12 \pm 0.26 \pm 0.81) \times 10^{-5}$	$(8.41 \pm 1.02 \pm 0.12 \pm 0.39 \pm 0.79) \times 10^{-5}$	[83]	
$B_s^0 \to D_s^{+(*)}D_s^{-(*)}$	$(3.36 \pm 0.11 \pm 0.14 \pm 0.09 \pm 0.38) \times 10^{-2}$	$(3.05 \pm 0.10 \pm 0.13 \pm 0.14 \pm 0.34) \times 10^{-2}$	[84]	
$B_s^0 \to D_s^{*\pm}D_s^{\mp}$	$(1.49 \pm 0.06 \pm 0.07 \pm 0.04 \pm 0.17) \times 10^{-2}$	$(1.35 \pm 0.06 \pm 0.06 \pm 0.06 \pm 0.15) \times 10^{-2}$	[84]	
$B_s^0 \to D_s^{*+}D_s^{*-}$	$(1.39 \pm 0.09 \pm 0.10 \pm 0.04 \pm 0.16) \times 10^{-2}$	$(1.27 \pm 0.08 \pm 0.09 \pm 0.06 \pm 0.14) \times 10^{-2}$	[84]	
$B_s^0 \to \overline{D}^0K_S^0$	$(4.69 \pm 0.51 \pm 0.28 \pm 0.15 \pm 0.64) \times 10^{-4}$	$(4.3 \pm 0.5 \pm 0.3 \pm 0.3 \pm 0.6) \times 10^{-4}$	[85]	
$B_s^0 \to \overline{D}^{*0}K_S^0$	$(3.05 \pm 1.13 \pm 0.40 \pm 0.10 \pm 0.41) \times 10^{-4}$	$(2.8 \pm 1.0 \pm 0.3 \pm 0.2 \pm 0.4) \times 10^{-4}$	[85]	
$B_s^0 \to \overline{D}^0\overline{K}^{*0}$	$(5.31 \pm 1.22 \pm 0.54 \pm 0.17 \pm 0.35) \times 10^{-4}$	$(4.72 \pm 1.07 \pm 0.48 \pm 0.37 \pm 0.74) \times 10^{-4}$	[86]	$\star$
$B_s^0 \to \overline{D}^0K^-\pi^+$	$(1.11 \pm 0.05 \pm 0.07 \pm 0.04 \pm 0.06) \times 10^{-3}$	$(1.00 \pm 0.04 \pm 0.06 \pm 0.08 \pm 0.10) \times 10^{-3}$	[87]	$\star$
$B_s^0 \to \overline{D}^0\phi$	$(3.25 \pm 0.38 \pm 0.19 \pm 0.11 \pm 0.18) \times 10^{-5}$	$(3.0 \pm 0.3 \pm 0.2 \pm 0.2 \pm 0.2) \times 10^{-5}$	[88]	$\star$
$B_s^0 \to \overline{D}^{*0}\phi$	$(4.01 \pm 0.48 \pm 0.27 \pm 0.13 \pm 0.23) \times 10^{-5}$	$(3.7 \pm 0.5 \pm 0.2 \pm 0.2 \pm 0.2) \times 10^{-5}$	[88]	$\star$
$B_s^0 \to \overline{D}^0K^+K^-$	$(6.13 \pm 0.59 \pm 0.28 \pm 0.20 \pm 0.56) \times 10^{-5}$	$(5.7 \pm 0.5 \pm 0.2 \pm 0.3 \pm 0.5) \times 10^{-5}$	[89]	$\star$
$B_s^0 \to D_s^{\mp}K^{\pm}$	$(2.41 \pm 0.05 \pm 0.06 \pm 0.14) \times 10^{-4}$	$(2.29 \pm 0.05 \pm 0.06 \pm 0.17) \times 10^{-4}$	[90]	$\star$
$B_s^0 \to D_s^-\pi^+\pi^-\pi^+$	$(6.43 \pm 1.18 \pm 0.64 \pm 0.38) \times 10^{-3}$	$(6.01 \pm 1.11 \pm 0.60 \pm 0.48) \times 10^{-3}$	[91]	$\star$
$B_s^0 \to D_s^-K^+\pi^-\pi^+$	$(3.34 \pm 0.32 \pm 0.19 \pm 0.73) \times 10^{-4}$	$(3.13 \pm 0.30 \pm 0.18 \pm 0.76) \times 10^{-4}$	[92]	$\star$
$B_s^0 \to D_{s1}(2536)^-\pi^+$	$(2.57 \pm 0.64 \pm 0.26 \pm 0.56) \times 10^{-5}$	$(2.41 \pm 0.60 \pm 0.24 \pm 0.58) \times 10^{-5}$	[92]	$\star$

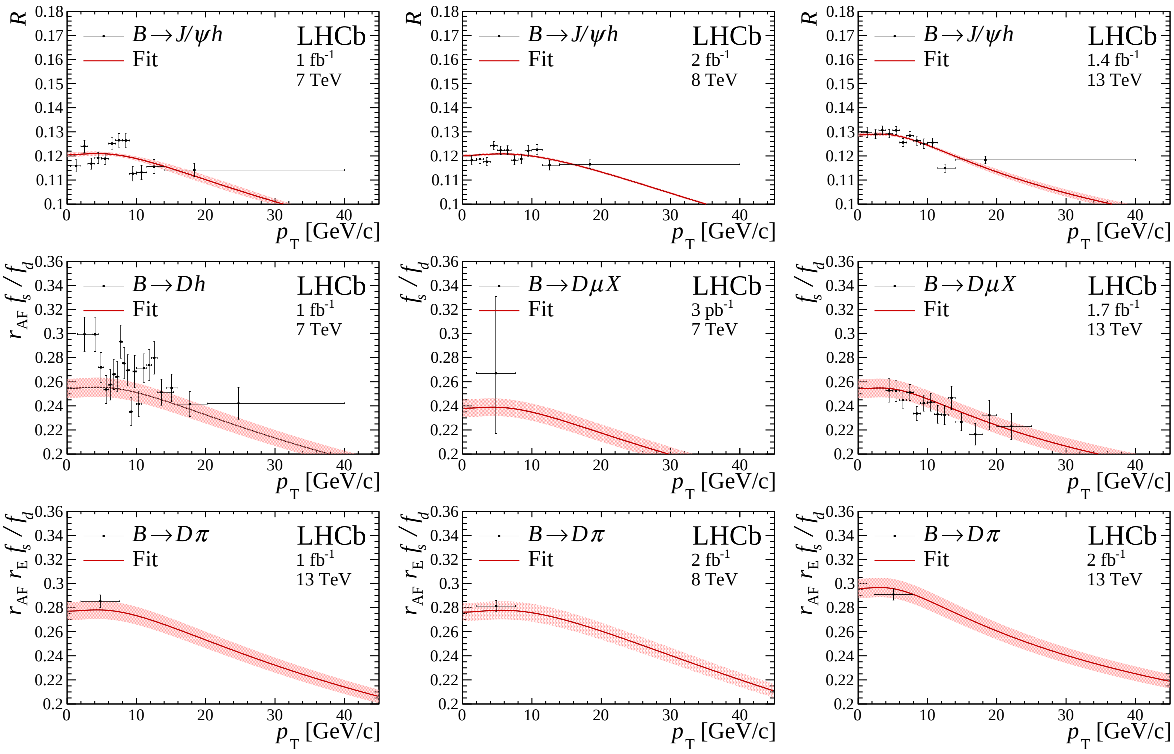

Figure 4: Measurements of f_s/f_d sensitive observables as a function of the B-meson transverse momentum, p_{T}, overlaid with the fit function. A Tsallis-statistics inspired function is used in this plot as described in the text. The scaling factors r_{AF} and r_E are defined in the text; the variable $\mathcal{R}$ is defined in Eq. 4. The vertical axes are zero-suppressed. The uncertainties on the data points are fully independent of each other; overall uncertainties for measurements in multiple p_{T} intervals are propagated through scaling parameters, as described in the text. The band associated with the fit function shows the uncertainty on the post-fit function for each sample.

Acknowledgements

We express our gratitude to our colleagues in the CERN accelerator departments for the excellent performance of the LHC. We thank the technical and administrative staff at the LHCb institutes. We acknowledge support from CERN and from the national agencies: CAPES, CNPq, FAPERJ and FINEP (Brazil); MOST and NSFC (China); CNRS/IN2P3 (France); BMBF, DFG and MPG (Germany); INFN (Italy); NWO (Netherlands); MNiSW and NCN (Poland); MEN/IFA (Romania); MSHE (Russia); MICINN (Spain); SNSF and SER (Switzerland); NASU (Ukraine); STFC (United Kingdom); DOE NP and NSF (USA). We acknowledge the computing resources that are provided by CERN, IN2P3 (France), KIT and DESY (Germany), INFN (Italy), SURF (Netherlands), PIC (Spain), GridPP (United Kingdom), RRCKI and Yandex LLC (Russia), CSCS (Switzerland), IFIN-HH (Romania), CBPF (Brazil), PL-GRID (Poland) and NERSC (USA). We are indebted to the communities behind the multiple open-source software packages on which we depend. Individual groups or members have received support from ARC and ARDC (Australia); AvH Foundation (Germany); EPLANET, Marie Skłodowska-Curie Actions and ERC (European Union); A*MIDEX, ANR, Labex P2IO and OCEVU, and Région Auvergne-Rhône-Alpes (France); Key Research Program of Frontier Sciences of CAS, CAS PIFI, CAS CCEPP, Fundamental Research Funds for the Central Universities, and Sci. & Tech. Program of Guangzhou (China); RFBR, RSF and Yandex LLC (Russia); GVA, XuntaGal and GENCAT (Spain); the Leverhulme Trust, the Royal Society and UKRI (United Kingdom).

A Supplemental material

Full results on the parameters for the default fit and the fit without external theory constraints are presented in Tables 7 and 8, respectively. The correlation matrices of the results for these fits also shown in Tables 9 and 10, respectively. This is important when considering the results at different energies, since they are correlated among each other.

The listed parameters are:

- a and b are the intercept and slope of the transverse-momentum-dependent functions at the three center-of-mass energies;
- r_{AF} and r_{E} are the scaling parameters with respect to the theoretical inputs;
- S_1 is the parameter propagating the correlated systematic uncertainty due to external parameters;
- S_2, S_3, and S_4 are the parameters propagating experimental systematic uncertainties.
- F_R is the ratio of the $B_s^0 \to J/\psi\phi$ to $B^+ \to J/\psi K^+$ branching fractions, as detailed in the text.

Table 7: Output parameters of the default fit to the data.

$a(7\,\mathrm{TeV})$	0.244 ± 0.008
$b(7\,\mathrm{TeV})$	$(-10.3 \pm 2.7) \times 10^{-4}$
S_1	1.009 ± 0.026
S_2	1.030 ± 0.028
r_{AF}	1.082 ± 0.032
$\mathcal{F}_R$	0.505 ± 0.016
$a(8\,\mathrm{TeV})$	0.240 ± 0.008
$b(8\,\mathrm{TeV})$	$(-3.5 \pm 2.3) \times 10^{-4}$
$a(13\,\mathrm{TeV})$	0.263 ± 0.008
$b(13\,\mathrm{TeV})$	$(-17.6 \pm 2.1) \times 10^{-4}$
S_3	0.997 ± 0.008
S_4	0.977 ± 0.021
r_{E}	1.071 ± 0.030

Table 8: Output parameters of the fit to the data without external theory constraints.

$a(7\,\mathrm{TeV})$	0.238 ± 0.008
$b(7\,\mathrm{TeV})$	$(-10.3 \pm 2.7) \times 10^{-4}$
S_1	1.000 ± 0.026
S_2	1.00 ± 0.04
r_{AF}	1.16 ± 0.06
$\mathcal{F}_R$	0.517 ± 0.017
$a(8\,\mathrm{TeV})$	0.234 ± 0.008
$b(8\,\mathrm{TeV})$	$(-3.3 \pm 2.3) \times 10^{-4}$
$a(13\,\mathrm{TeV})$	0.256 ± 0.009
$b(13\,\mathrm{TeV})$	$(-16.9 \pm 2.0) \times 10^{-4}$
S_3	1.000 ± 0.009
S_4	0.998 ± 0.023
r_{E}	1.04 ± 0.04

Table 9: Output correlation matrix of the default fit versus p_{T}.

	$a(7\,\mathrm{TeV})$	$b(7\,\mathrm{TeV})$	S_1	S_2	r_{AF}	$\mathcal{F}_R$	$a(8\,\mathrm{TeV})$	$b(8\,\mathrm{TeV})$	$a(13\,\mathrm{TeV})$	$b(13\,\mathrm{TeV})$	S_3	S_4	r_{E}
$a(7\,\mathrm{TeV})$	1.000	−0.360	−0.589	−0.185	−0.318	−0.955	0.925	−0.046	0.933	−0.314	−0.223	−0.645	−0.198
$b(7\,\mathrm{TeV})$		1.000	0.067	−0.045	−0.003	0.131	−0.129	0.010	−0.130	0.048	0.034	0.097	0.109
S_1			1.000	−0.075	−0.128	0.615	−0.596	0.029	−0.601	0.170	0.022	0.064	−0.079
S_2				1.000	−0.542	0.193	−0.184	0.004	−0.186	0.068	0.083	0.239	0.841
r_{AF}					1.000	0.328	−0.320	0.019	−0.322	0.129	0.142	0.410	−0.569
$\mathcal{F}_R$						1.000	−0.967	0.044	−0.976	0.326	0.233	0.676	0.198
$a(8\,\mathrm{TeV})$							1.000	−0.257	0.945	−0.318	−0.226	−0.654	−0.202
$b(8\,\mathrm{TeV})$								1.000	−0.046	0.021	0.010	0.030	0.030
$a(13\,\mathrm{TeV})$									1.000	−0.492	−0.228	−0.660	−0.202
$b(13\,\mathrm{TeV})$										1.000	0.056	0.161	0.098
S_3											1.000	−0.059	0.087
S_4												1.000	0.251
r_{E}													1.000

Table 10: Output correlation matrix of the fit versus p_{T} without theory constraints.

	$a(7\,\mathrm{TeV})$	$b(7\,\mathrm{TeV})$	S_1	S_2	r_{AF}	$\mathcal{F}_R$	$a(8\,\mathrm{TeV})$	$b(8\,\mathrm{TeV})$	$a(13\,\mathrm{TeV})$	$b(13\,\mathrm{TeV})$	S_3	S_4	r_{E}
$a(7\,\mathrm{TeV})$	1.000	−0.343	−0.525	0.001	−0.367	−0.958	0.931	−0.049	0.938	−0.333	−0.257	−0.672	−0.002
$b(7\,\mathrm{TeV})$		1.000	0.069	0.000	−0.032	0.125	−0.123	0.011	−0.124	0.048	0.034	0.088	0.111
S_1			1.000	0.000	−0.166	0.548	−0.531	0.027	−0.536	0.150	0.003	0.007	0.000
S_2				1.000	−0.768	−0.001	0.001	−0.000	0.001	−0.000	−0.000	−0.001	0.920
r_{AF}					1.000	0.378	−0.367	0.019	−0.370	0.152	0.178	0.467	−0.787
$\mathcal{F}_R$						1.000	−0.970	0.048	−0.978	0.343	0.267	0.701	−0.004
$a(8\,\mathrm{TeV})$							1.000	−0.252	0.949	−0.336	−0.260	−0.680	−0.005
$b(8\,\mathrm{TeV})$								1.000	−0.049	0.023	0.013	0.034	0.018
$a(13\,\mathrm{TeV})$									1.000	−0.502	−0.262	−0.686	−0.004
$b(13\,\mathrm{TeV})$										1.000	0.073	0.191	0.018
S_3											1.000	0.004	−0.000
S_4												1.000	−0.001
r_{E}													1.000

References

[1] OPAL collaboration, P. D. Acton *et al.*, *Evidence for the existence of the strange b-flavoured meson B_s^0 in Z^0 decays*, Phys. Lett. **B295** (1992) 357 .

[2] ALEPH collaboration, D. Buskulic *et al.*, *Measurement of the B_s^0 lifetime and production rate with $D_s^-\ell^+$ combinations in Z decays*, Phys. Lett. **B361** (1995) 221.

[3] L3 collaboration, M. Acciarri *et al.*, *Measurements of the $b\bar{b}$ production cross-section and forward-backward asymmetry at centre-of-mass energies above the Z pole at LEP*, Phys. Lett. **B485** (2000) 71, `arXiv:hep-ex/0005023`.

[4] DELPHI collaboration, J. Abdallah *et al.*, *A Measurement of the branching fractions of the b quark into charged and neutral b hadrons*, Phys. Lett. **B576** (2003) 29, `arXiv:hep-ex/0311005`.

[5] CDF collaboration, T. Aaltonen *et al.*, *Measurement of ratios of fragmentation fractions for bottom hadrons in $p\bar{p}$ collisions at $\sqrt{s}$ = 1.96 TeV*, Phys. Rev. **D77** (2008) 072003, `arXiv:0801.4375`.

[6] Heavy Flavor Averaging Group, Y. Amhis *et al.*, *Averages of b-hadron, c-hadron, and τ-lepton properties as of 2018*, `arXiv:1909.12524`, updated results and plots available at `https://hflav.web.cern.ch`.

[7] Particle Data Group, P. A. Zyla *et al.*, *Review of particle physics*, Prog. Theor. Exp. Phys. **2020** (2020) 083C01.

[8] LHCb collaboration, R. Aaij *et al.*, *Measurement of b hadron production fractions in 7 TeV pp collisions*, Phys. Rev. **D85** (2012) 032008, `arXiv:1111.2357`.

[9] LHCb collaboration, R. Aaij *et al.*, *Measurement of the fragmentation fraction ratio f_s/f_d and its dependence on B meson kinematics*, JHEP **04** (2013) 001, `arXiv:1301.5286`.

[10] LHCb collaboration, R. Aaij *et al.*, *Measurement of f_s/f_u variation with proton-proton collision energy and B-meson kinematics*, Phys. Rev. Lett. **124** (2020) 122002, `arXiv:1910.09934`.

[11] LHCb collaboration, R. Aaij *et al.*, *Analysis of the resonant components in $\overline{B}_s^0 \to J/\psi\pi^+\pi^-$*, Phys. Rev. **D86** (2012) 052006, `arXiv:1204.5643`.

[12] LHCb collaboration, R. Aaij *et al.*, *Measurement of relative branching fractions of B decays to $\psi(2S)$ and J/ψ mesons*, Eur. Phys. J. **C72** (2012) 2118, `arXiv:1205.0918`.

[13] LHCb collaboration, R. Aaij *et al.*, *Differential branching fraction and angular analysis of the $B^+ \to K^+\mu^+\mu^-$ decay*, JHEP **02** (2013) 105, `arXiv:1209.4284`.

[14] LHCb collaboration, R. Aaij *et al.*, *Angular analysis and differential branching fraction of the decay $B_s^0 \to \phi\mu^+\mu^-$*, JHEP **09** (2015) 179, `arXiv:1506.08777`.

[15] LHCb collaboration, R. Aaij *et al.*, *Observation of the $B_s^0 \to J/\psi\phi\phi$ decay*, JHEP **03** (2016) 040, `arXiv:1601.05284`.

[16] LHCb collaboration, R. Aaij *et al.*, *Amplitude analysis and branching fraction measurement of $\overline{B}{}^0_s \to J/\psi K^+K^-$*, Phys. Rev. **D87** (2013) 072004, `arXiv:1302.1213`.

[17] Belle collaboration, F. Thorne *et al.*, *Measurement of the decays $B^0_s \to J/\psi\phi(1020)$, $B^0_s \to J/\psi f_2'(1525)$ and $B^0_s \to J/\psi K^+K^-$ at Belle*, Phys. Rev. **D88** (2013) 114006, `arXiv:1309.0704`.

[18] CDF collaboration, F. Abe *et al.*, *Ratios of bottom meson branching fractions involving J/ψ mesons and determination of b quark fragmentation fractions*, Phys. Rev. **D54** (1996) 6596, `arXiv:hep-ex/9607003`.

[19] M. Bordone *et al.*, *A puzzle in $\bar{B}^0_{(s)} \to D^+_{(s)}\{\pi^-, K^-\}$ decays and extraction of the f_s/f_d fragmentation fraction*, Eur. Phys. J. **C80** (2020) 951, `arXiv:2007.10338`.

[20] LHCb collaboration, R. Aaij *et al.*, *Measurements of the branching fractions of the decays $B^0_s \to D^\mp_s K^\pm$ and $B^0_s \to D^-_s\pi^+$*, JHEP **06** (2012) 115, `arXiv:1204.1237`.

[21] Belle collaboration, R. Louvot *et al.*, *Measurement of the decay $B^0_s \to D^-_s\pi^+$ and evidence for $B^0_s \to D^\mp_s K^\pm$ in e^+e^- annihilation at $\sqrt{s} \sim 10.87$ GeV*, Phys. Rev. Lett. **102** (2009) 021801, `arXiv:0809.2526`.

[22] CDF collaboration, A. Abulencia *et al.*, *Measurement of the ratios of branching fractions $B(B^0_{(s)} \to D^-_{(s)}\pi^+\pi^+\pi^-)/B(B^0 \to D^-\pi^+\pi^+\pi^-)$ and $B(B^0_{(s)} \to D^-_{(s)}\pi^+)/B(B^0 \to D^-\pi^+)$*, Phys. Rev. Lett. **98** (2007) 061802, `arXiv:hep-ex/0610045`.

[23] LHCb collaboration, R. Aaij *et al.*, *Measurement of b-hadron fractions in 13 TeV pp collisions*, Phys. Rev. **D100** (2019) 031102(R), `arXiv:1902.06794`.

[24] LHCb collaboration, R. Aaij *et al.*, *Branching fraction measurement of the $B^0 \to D^+_s\pi^-$ decay*, `arXiv:2010.11986`, submitted to Eur. Phys. J. C.

[25] LHCb collaboration, *Updated average f_s/f_d b-hadron production fraction ratio for 7 TeV pp collisions*, LHCb-CONF-2013-011, 2013.

[26] LHCb collaboration, A. A. Alves Jr. *et al.*, *The LHCb detector at the LHC*, JINST **3** (2008) S08005.

[27] LHCb collaboration, R. Aaij *et al.*, *LHCb detector performance*, Int. J. Mod. Phys. **A30** (2015) 1530022, `arXiv:1412.6352`.

[28] T. Sjöstrand, S. Mrenna, and P. Skands, *A brief introduction to PYTHIA 8.1*, Comput. Phys. Commun. **178** (2008) 852, `arXiv:0710.3820`.

[29] I. Belyaev *et al.*, *Handling of the generation of primary events in Gauss, the LHCb simulation framework*, J. Phys. Conf. Ser. **331** (2011) 032047.

[30] D. J. Lange, *The EvtGen particle decay simulation package*, Nucl. Instrum. Meth. **A462** (2001) 152.

[31] N. Davidson, T. Przedzinski, and Z. Was, *PHOTOS interface in C++: Technical and physics documentation*, Comp. Phys. Comm. **199** (2016) 86, `arXiv:1011.0937`.

[32] Geant4 collaboration, J. Allison *et al.*, *Geant4 developments and applications*, IEEE Trans. Nucl. Sci. **53** (2006) 270; Geant4 collaboration, S. Agostinelli *et al.*, *Geant4: A simulation toolkit*, Nucl. Instrum. Meth. **A506** (2003) 250.

[33] M. Clemencic *et al.*, *The LHCb simulation application, Gauss: Design, evolution and experience*, J. Phys. Conf. Ser. **331** (2011) 032023.

[34] I. I. Bigi, T. Mannel, and N. Uraltsev, *Semileptonic width ratios among beauty hadrons*, JHEP **09** (2011) 012, `arXiv:1105.4574`.

[35] LHCb collaboration, R. Aaij *et al.*, *Measurement of the b-quark production cross-section in 7 and 13 TeV pp collisions*, Phys. Rev. Lett. **118** (2017) 052002, Erratum ibid. **119** (2017) 169901, `arXiv:1612.05140`.

[36] R. Fleischer, N. Serra, and N. Tuning, *A new strategy for B_s branching ratio measurements and the search for New Physics in $B_s^0 \to \mu^+\mu^-$*, Phys. Rev. **D82** (2010) 034038, `arXiv:1004.3982`.

[37] R. Fleischer, N. Serra, and N. Tuning, *Tests of factorization and SU(3) relations in B decays into heavy-light final states*, Phys. Rev. **D83** (2011) 014017, `arXiv:1012.2784`.

[38] ATLAS collaboration, G. Aad *et al.*, *Determination of the ratio of b-quark fragmentation fractions f_s/f_d in pp collisions at $\sqrt{s} = 7$ TeV with the ATLAS detector*, Phys. Rev. Lett. **115** (2015) 262001, `arXiv:1507.08925`.

[39] X. Liu, W. Wang, and Y. Xie, *Penguin pollution in $B \to J/\psi V$ decays and impact on the extraction of the $B_s - \bar{B}_s$ mixing phase*, Phys. Rev. **D89** (2014) 094010, `arXiv:1309.0313`.

[40] BESIII, M. Ablikim *et al.*, *Amplitude analysis and branching fraction measurement of $D_s^+ \to K^+K^-\pi^+$*, `arXiv:2011.08041`.

[41] M. Bordone, N. Gubernari, D. van Dyk, and M. Jung, *Heavy-Quark expansion for $\bar{B}_s \to D_s^{(*)}$ form factors and unitarity bounds beyond the $SU(3)_F$ limit*, Eur. Phys. J. **C80** (2020) 347, `arXiv:1912.09335`.

[42] G. D'Agostini, *On the use of the covariance matrix to fit correlated data*, Nucl. Instrum. Meth. **A346** (1994) 306.

[43] X.-H. Mo, *Unbiased χ^2 estimator for linear function fit involving correlated data*, HEPNP **31** (2007) 745.

[44] A. V. Berezhnoy and A. K. Likhoded, *Relative yield of heavy hadrons as a function of the transverse momentum in LHC experiments*, Phys. Atom. Nucl. **78** (2015) 292.

[45] G. W. Snedecor and W. G. Cochran, *Statistical Methods*, Wiley, 1991.

[46] K. De Bruyn *et al.*, *Branching Ratio Measurements of B_s Decays*, Phys. Rev. **D86** (2012) 014027, `arXiv:1204.1735`.

[47] F. Dettori and D. Guadagnoli, *On the model dependence of measured B_s-meson branching fractions*, Phys. Lett. **B784** (2018) 96, `arXiv:1804.03591`.

[48] LHCb collaboration, R. Aaij *et al.*, *Updated measurement of time-dependent CP-violating observables in $B_s^0 \to J/\psi K^+K^-$ decays*, Eur. Phys. J. **C79** (2019) 706, Erratum ibid. **C80** (2020) 601, arXiv:1906.08356.

[49] M. Jung, *Branching ratio measurements and isospin violation in B-meson decays*, Phys. Lett. B **753** (2016) 187, arXiv:1510.03423.

[50] Belle collaboration, K. Chilikin *et al.*, *Observation of a new charged charmoniumlike state in $\bar{B}^0 \to J/\psi K^-\pi^+$ decays*, Phys. Rev. **D90** (2014) 112009, arXiv:1408.6457.

[51] LHCb collaboration, *Combination of the ATLAS, CMS and LHCb results on the $B^0_{(s)} \to \mu^+\mu^-$ decays*, LHCb-CONF-2020-002, 2020, ATLAS-CONF-2020-049, CMS PAS BPH-20-003, LHCb-CONF-2020-002.

[52] LHCb collaboration, R. Aaij *et al.*, *Measurement of $|V_{cb}|$ with $B_s^0 \to D_s^{(*)-}\mu^+\nu$ decays*, Phys. Rev. **D100** (2020) 072004, arXiv:2001.03225.

[53] I. Caprini, L. Lellouch, and M. Neubert, *Dispersive bounds on the shape of $B \to D^{(*)}\ell\nu$ form factors*, Nucl. Phys. **B530** (1998) 153, arXiv:hep-ph/9712417.

[54] C. G. Boyd, B. Grinstein, and R. F. Lebed, *Constraints on form-factors for exclusive semileptonic heavy to light meson decays*, Phys. Rev. Lett. **74** (1995) 4603, arXiv:hep-ph/9412324.

[55] LHCb collaboration, R. Aaij *et al.*, *Measurement of the ratio of branching fractions $\mathcal{B}(B^0 \to K^{*0}\gamma)/\mathcal{B}(B_s^0 \to \phi\gamma)$ and the direct CP asymmetry in $B^0 \to K^{*0}\gamma$*, Nucl. Phys. **B867** (2013) 1, arXiv:1209.0313.

[56] LHCb collaboration, R. Aaij *et al.*, *Measurement of the $B_s^0 \to \mu^+\mu^-$ branching fraction and effective lifetime and search for $B^0 \to \mu^+\mu^-$ decays*, Phys. Rev. Lett. **118** (2017) 191801, arXiv:1703.05747.

[57] LHCb collaboration, R. Aaij *et al.*, *Evidence for the decay $B_s^0 \to \overline{K}^{*0}\mu^+\mu^-$*, JHEP **07** (2018) 020, arXiv:1804.07167.

[58] LHCb collaboration, R. Aaij *et al.*, *Study of the rare B_s^0 and B^0 decays into the $\pi^+\pi^-\mu^+\mu^-$ final state*, Phys. Lett. **B743** (2015) 46, arXiv:1412.6433.

[59] LHCb collaboration, R. Aaij *et al.*, *Measurement of the time-dependent CP asymmetries in $B_s^0 \to J/\psi K^0_S$*, JHEP **06** (2015) 131, arXiv:1503.07055.

[60] LHCb collaboration, R. Aaij *et al.*, *Observation of the $B_s^0 \to J/\psi K^0_S K^\pm\pi^\mp$ decay*, JHEP **07** (2014) 140, arXiv:1405.3219.

[61] LHCb collaboration, R. Aaij *et al.*, *Observation of the decay $\overline{B}{}_s^0 \to \psi(2S)K^+\pi^-$*, Phys. Lett. **B747** (2015) 484, arXiv:1503.07112.

[62] LHCb collaboration, R. Aaij *et al.*, *Evidence for the decay $B^0 \to J/\psi\omega$ and measurement of the relative branching fractions of B_s^0 meson decays to $J/\psi\eta$ and $J/\psi\eta'$*, Nucl. Phys. **B867** (2013) 547, arXiv:1210.2631.

[63] LHCb collaboration, R. Aaij *et al.*, *Observation of $B_s^0 \to \chi_{c1}\phi$ decay and study of $B^0 \to \chi_{c1,2}K^{*0}$ decays*, Nucl. Phys. **B874** (2013) 663, `arXiv:1305.6511`.

[64] LHCb collaboration, R. Aaij *et al.*, *Measurement of CP violation parameters and polarisation fractions in $B_s^0 \to J/\psi \overline{K}^{*0}$ decays*, JHEP **11** (2015) 082, `arXiv:1509.00400`.

[65] LHCb collaboration, R. Aaij *et al.*, *Observation of $B_{(s)}^0 \to J/\psi p\overline{p}$ decays and precision measurements of the $B_{(s)}^0$ masses*, Phys. Rev. Lett. **122** (2019) 191804, `arXiv:1902.05588`.

[66] LHCb collaboration, R. Aaij *et al.*, *Observations of $B_s^0 \to \psi(2S)\eta$ and $B_{(s)}^0 \to \psi(2S)\pi^+\pi^-$ decays*, Nucl. Phys. **B871** (2013) 403, `arXiv:1302.6354`.

[67] LHCb collaboration, R. Aaij *et al.*, *Study of η–η' mixing from measurement of $B_{(s)}^0 \to J/\psi\eta^{(\prime)}$ decay rates*, JHEP **01** (2015) 024, `arXiv:1411.0943`.

[68] LHCb collaboration, R. Aaij *et al.*, *Observation of $\overline{B}_s^0 \to J/\psi f_1(1285)$ decays and measurement of the $f_1(1285)$ mixing angle*, Phys. Rev. Lett. **112** (2014) 091802, `arXiv:1310.2145`.

[69] LHCb collaboration, R. Aaij *et al.*, *Observation of the annihilation decay mode $B^0 \to K^+K^-$*, Phys. Rev. Lett. **118** (2017) 081801, `arXiv:1610.08288`.

[70] LHCb collaboration, R. Aaij *et al.*, *Measurement of b-hadron branching fractions for two-body decays into charmless charged hadrons*, JHEP **10** (2012) 037, `arXiv:1206.2794`.

[71] LHCb collaboration, R. Aaij *et al.*, *Measurement of the branching fraction of the decay $B_s^0 \to K_S^0 K_S^0$*, Phys. Rev. **D102** (2020) 012011, `arXiv:2002.08229`.

[72] LHCb collaboration, R. Aaij *et al.*, *Updated branching fraction measurements of $B_{(s)}^0 \to K_S^0 h^+ h'^-$ decays*, JHEP **11** (2017) 027, `arXiv:1707.01665`.

[73] LHCb collaboration, R. Aaij *et al.*, *First observation of the decay $B_s^0 \to K^{*0}\overline{K}^{*0}$*, Phys. Lett. **B709** (2012) 50, `arXiv:1111.4183`.

[74] LHCb collaboration, R. Aaij *et al.*, *Observation of $B_s^0 \to K^{*\pm}K^{\mp}$ and evidence of $B_s^0 \to K^{*-}\pi^+$ decays*, New J. Phys. **16** (2014) 123001, `arXiv:1407.7704`.

[75] LHCb collaboration, R. Aaij *et al.*, *Observation of charmless baryonic decays $B_{(s)}^0 \to p\overline{p}h^+h'^-$*, Phys. Rev. **D96** (2017) 051103, `arXiv:1704.08497`.

[76] LHCb collaboration, R. Aaij *et al.*, *First observation of a baryonic B_s^0 decay*, Phys. Rev. Lett. **119** (2017) 041802, `arXiv:1704.07908`.

[77] LHCb collaboration, R. Aaij *et al.*, *First observation of the decay $B_s^0 \to \phi\overline{K}^{*0}$*, JHEP **11** (2013) 092, `arXiv:1306.2239`.

[78] LHCb collaboration, R. Aaij *et al.*, *Measurement of the $B_s^0 \to \phi\phi$ branching fraction and search for the decay $B^0 \to \phi\phi$*, JHEP **10** (2015) 053, `arXiv:1508.00788`.

[79] LHCb collaboration, R. Aaij *et al.*, *Observation of the decays $B_s^0 \to \phi\pi^+\pi^-$ and $B^0 \to \phi\pi^+\pi^-$*, Phys. Rev. **D95** (2017) 012006, arXiv:1610.05187.

[80] LHCb collaboration, R. Aaij *et al.*, *Study of charmonium production in b-hadron decays and first evidence for the decay $B_s^0 \to \phi\phi\phi$*, Eur. Phys. J. **C77** (2017) 609, arXiv:1706.07013.

[81] LHCb collaboration, R. Aaij *et al.*, *Study of beauty hadron decays into pairs of charm hadrons*, Phys. Rev. Lett. **112** (2014) 202001, arXiv:1403.3606.

[82] LHCb collaboration, R. Aaij *et al.*, *First observations of $\overline{B}_s^0 \to D^+D^-, D_s^+D^-$ and $D^0\overline{D}^0$ decays*, Phys. Rev. **D87** (2013) 092007, arXiv:1302.5854.

[83] LHCb collaboration, R. Aaij *et al.*, *Observation of the $B_s^0 \to D^{*\pm}D^{\mp}$ decay*, arXiv:2012.11341, to appear in JHEP.

[84] LHCb collaboration, R. Aaij *et al.*, *Measurement of the $B_s^0 \to D_s^{(*)+}D_s^{(*)-}$ branching fractions*, Phys. Rev. **D93** (2016) 092008, arXiv:1602.07543.

[85] LHCb collaboration, R. Aaij *et al.*, *Observation of $B_s^0 \to \overline{D}^0 K_S^0$ and evidence for $B_s^0 \to \overline{D}^{*0} K_S^0$ decays*, Phys. Rev. Lett. **116** (2016) 161802, arXiv:1603.02408.

[86] LHCb collaboration, R. Aaij *et al.*, *First observation of the decay $\overline{B}_s^0 \to D^0 K^{*0}$ and a measurement of the ratio of branching fractions $\frac{\mathcal{B}(\overline{B}_s^0 \to D^0 K^{*0})}{\mathcal{B}(B^0 \to D^0 \rho^0)}$*, Phys. Lett. **B706** (2011) 32, arXiv:1110.3676.

[87] LHCb collaboration, R. Aaij *et al.*, *Measurements of the branching fractions of the decays $B_s^0 \to \overline{D}^0 K^-\pi^+$ and $B^0 \to \overline{D}^0 K^+\pi^-$*, Phys. Rev. **D87** (2013) 112009, arXiv:1304.6317.

[88] LHCb collaboration, R. Aaij *et al.*, *Observation of the decay $B_s^0 \to \overline{D}^{*0}\phi$ and search for the mode $B^0 \to \overline{D}^0\phi$*, Phys. Rev. **D98** (2018) 071103(R), arXiv:1807.01892.

[89] LHCb collaboration, R. Aaij *et al.*, *Observation of the decay $B_s^0 \to \overline{D}^0 K^+K^-$*, Phys. Rev. **D98** (2018) 072006, arXiv:1807.01891.

[90] LHCb collaboration, R. Aaij *et al.*, *Determination of the branching fractions of $B_s^0 \to D_s^{\mp}K^{\pm}$ and $B^0 \to D_s^- K^+$*, JHEP **02** (2015) 029, arXiv:1412.7654.

[91] LHCb collaboration, R. Aaij *et al.*, *Measurements of the branching fractions for $B_{(s)}^0 \to D_{(s)}\pi\pi\pi$ and $\Lambda_b^0 \to \Lambda_c^+\pi\pi\pi$*, Phys. Rev. **D84** (2011) 092001, Erratum ibid. **D85** (2012) 039904, arXiv:1109.6831.

[92] LHCb collaboration, R. Aaij *et al.*, *First observation of the decays $\overline{B}_{(s)}^0 \to D_s^+K^-\pi^+\pi^-$ and $\overline{B}_s^0 \to D_{s1}(2536)^+\pi^-$*, Phys. Rev. **D86** (2012) 112005, arXiv:1211.1541.

[93] C. Tsallis, *Possible generalization of Boltzmann-Gibbs statistics*, J. Statist. Phys. **52** (1988) 479.

[94] C. Tsallis, *Nonextensive statistics: Theoretical, experimental and computational evidences and connections*, Braz. J. Phys. **29** (1999) 1.

[95] STAR collaboration, B. I. Abelev *et al.*, *Strange particle production in p+p collisions at $\sqrt{s} = 200$ GeV*, Phys. Rev. **C75** (2007) 064901, arXiv:nucl-ex/0607033.

[96] PHENIX collaboration, A. Adare *et al.*, *Identified charged hadron production in $p + p$ collisions at $\sqrt{s} = 200$ and 62.4 GeV*, Phys. Rev. **C83** (2011) 064903, arXiv:1102.0753.

[97] ALICE collaboration, K. Aamodt *et al.*, *Production of pions, kaons and protons in pp collisions at $\sqrt{s} = 900$ GeV with ALICE at the LHC*, Eur. Phys. J. **C71** (2011) 1655, arXiv:1101.4110.

[98] CMS collaboration, V. Khachatryan *et al.*, *Strange particle production in pp collisions at $\sqrt{s} = 0.9$ and 7 TeV*, JHEP **05** (2011) 064, arXiv:1102.4282.

[99] ATLAS collaboration, G. Aad *et al.*, *Charged-particle multiplicities in pp interactions measured with the ATLAS detector at the LHC*, New J. Phys. **13** (2011) 053033, arXiv:1012.5104.

LHCb collaboration

R. Aaij[32], C. Abellán Beteta[50], T. Ackernley[60], B. Adeva[46], M. Adinolfi[54], H. Afsharnia[9], C.A. Aidala[85], S. Aiola[25], Z. Ajaltouni[9], S. Akar[65], J. Albrecht[15], F. Alessio[48], M. Alexander[59], A. Alfonso Albero[45], Z. Aliouche[62], G. Alkhazov[38], P. Alvarez Cartelle[55], S. Amato[2], Y. Amhis[11], L. An[48], L. Anderlini[22], A. Andreianov[38], M. Andreotti[21], F. Archilli[17], A. Artamonov[44], M. Artuso[68], K. Arzymatov[42], E. Aslanides[10], M. Atzeni[50], B. Audurier[12], S. Bachmann[17], M. Bachmayer[49], J.J. Back[56], S. Baker[61], P. Baladron Rodriguez[46], V. Balagura[12], W. Baldini[21,48], J. Baptista Leite[1], R.J. Barlow[62], S. Barsuk[11], W. Barter[61], M. Bartolini[24], F. Baryshnikov[82], J.M. Basels[14], G. Bassi[29], B. Batsukh[68], A. Battig[15], A. Bay[49], M. Becker[15], F. Bedeschi[29], I. Bediaga[1], A. Beiter[68], V. Belavin[42], S. Belin[27], V. Bellee[49], K. Belous[44], I. Belov[40], I. Belyaev[41], G. Bencivenni[23], E. Ben-Haim[13], A. Berezhnoy[40], R. Bernet[50], D. Berninghoff[17], H.C. Bernstein[68], C. Bertella[48], A. Bertolin[28], C. Betancourt[50], F. Betti[20,d], Ia. Bezshyiko[50], S. Bhasin[54], J. Bhom[35], L. Bian[73], M.S. Bieker[15], S. Bifani[53], P. Billoir[13], M. Birch[61], F.C.R. Bishop[55], A. Bitadze[62], A. Bizzeti[22,k], M. Bjørn[63], M.P. Blago[48], T. Blake[56], F. Blanc[49], S. Blusk[68], D. Bobulska[59], J.A. Boelhauve[15], O. Boente Garcia[46], T. Boettcher[64], A. Boldyrev[81], A. Bondar[43], N. Bondar[38,48], S. Borghi[62], M. Borisyak[42], M. Borsato[17], J.T. Borsuk[35], S.A. Bouchiba[49], T.J.V. Bowcock[60], A. Boyer[48], C. Bozzi[21], M.J. Bradley[61], S. Braun[66], A. Brea Rodriguez[46], M. Brodski[48], J. Brodzicka[35], A. Brossa Gonzalo[56], D. Brundu[27], A. Buonaura[50], C. Burr[48], A. Bursche[27], A. Butkevich[39], J.S. Butter[32], J. Buytaert[48], W. Byczynski[48], S. Cadeddu[27], H. Cai[73], R. Calabrese[21,f], L. Calefice[15,13], L. Calero Diaz[23], S. Cali[23], R. Calladine[53], M. Calvi[26,j], M. Calvo Gomez[84], P. Camargo Magalhaes[54], A. Camboni[45,84], P. Campana[23], A.F. Campoverde Quezada[6], S. Capelli[26,j], L. Capriotti[20,d], A. Carbone[20,d], G. Carboni[31], R. Cardinale[24,h], A. Cardini[27], I. Carli[4], P. Carniti[26,j], L. Carus[14], K. Carvalho Akiba[32], A. Casais Vidal[46], G. Casse[60], M. Cattaneo[48], G. Cavallero[48], S. Celani[49], J. Cerasoli[10], A.J. Chadwick[60], M.G. Chapman[54], M. Charles[13], Ph. Charpentier[48], G. Chatzikonstantinidis[53], C.A. Chavez Barajas[60], M. Chefdeville[8], C. Chen[3], S. Chen[27], A. Chernov[35], V. Chobanova[46], S. Cholak[49], M. Chrzaszcz[35], A. Chubykin[38], V. Chulikov[38], P. Ciambrone[23], M.F. Cicala[56], X. Cid Vidal[46], G. Ciezarek[48], P.E.L. Clarke[58], M. Clemencic[48], H.V. Cliff[55], J. Closier[48], J.L. Cobbledick[62], V. Coco[48], J.A.B. Coelho[11], J. Cogan[10], E. Cogneras[9], L. Cojocariu[37], P. Collins[48], T. Colombo[48], L. Congedo[19,c], A. Contu[27], N. Cooke[53], G. Coombs[59], G. Corti[48], C.M. Costa Sobral[56], B. Couturier[48], D.C. Craik[64], J. Crkovská[67], M. Cruz Torres[1], R. Currie[58], C.L. Da Silva[67], E. Dall'Occo[15], J. Dalseno[46], C. D'Ambrosio[48], A. Danilina[41], P. d'Argent[48], A. Davis[62], O. De Aguiar Francisco[62], K. De Bruyn[78], S. De Capua[62], M. De Cian[49], J.M. De Miranda[1], L. De Paula[2], M. De Serio[19,c], D. De Simone[50], P. De Simone[23], J.A. de Vries[79], C.T. Dean[67], D. Decamp[8], L. Del Buono[13], B. Delaney[55], H.-P. Dembinski[15], A. Dendek[34], V. Denysenko[50], D. Derkach[81], O. Deschamps[9], F. Desse[11], F. Dettori[27,e], B. Dey[73], P. Di Nezza[23], S. Didenko[82], L. Dieste Maronas[46], H. Dijkstra[48], V. Dobishuk[52], A.M. Donohoe[18], F. Dordei[27], A.C. dos Reis[1], L. Douglas[59], A. Dovbnya[51], A.G. Downes[8], K. Dreimanis[60], M.W. Dudek[35], L. Dufour[48], V. Duk[77], P. Durante[48], J.M. Durham[67], D. Dutta[62], M. Dziewiecki[17], A. Dziurda[35], A. Dzyuba[38], S. Easo[57], U. Egede[69], V. Egorychev[41], S. Eidelman[43,v], S. Eisenhardt[58], S. Ek-In[49], L. Eklund[59,w], S. Ely[68], A. Ene[37], E. Epple[67], S. Escher[14], J. Eschle[50], S. Esen[32], T. Evans[48], A. Falabella[20], J. Fan[3], Y. Fan[6], B. Fang[73], S. Farry[60], D. Fazzini[26,j], P. Fedin[41], M. Féo[48], P. Fernandez Declara[48], A. Fernandez Prieto[46], J.M. Fernandez-tenllado Arribas[45], F. Ferrari[20,d], L. Ferreira Lopes[49], F. Ferreira Rodrigues[2], S. Ferreres Sole[32], M. Ferrillo[50], M. Ferro-Luzzi[48], S. Filippov[39], R.A. Fini[19], M. Fiorini[21,f], M. Firlej[34], K.M. Fischer[63], C. Fitzpatrick[62], T. Fiutowski[34], F. Fleuret[12], M. Fontana[13], F. Fontanelli[24,h], R. Forty[48], V. Franco Lima[60], M. Franco Sevilla[66], M. Frank[48], E. Franzoso[21], G. Frau[17], C. Frei[48], D.A. Friday[59], J. Fu[25], Q. Fuehring[15], W. Funk[48], E. Gabriel[32],

T. Gaintseva[42], A. Gallas Torreira[46], D. Galli[20,d], S. Gambetta[58,48], Y. Gan[3], M. Gandelman[2], P. Gandini[25], Y. Gao[5], M. Garau[27], L.M. Garcia Martin[56], P. Garcia Moreno[45], J. García Pardiñas[26,j], B. Garcia Plana[46], F.A. Garcia Rosales[12], L. Garrido[45], C. Gaspar[48], R.E. Geertsema[32], D. Gerick[17], L.L. Gerken[15], E. Gersabeck[62], M. Gersabeck[62], T. Gershon[56], D. Gerstel[10], Ph. Ghez[8], V. Gibson[55], H.K. Giemza[36], M. Giovannetti[23,p], A. Gioventù[46], P. Gironella Gironell[45], L. Giubega[37], C. Giugliano[21,f,48], K. Gizdov[58], E.L. Gkougkousis[48], V.V. Gligorov[13], C. Göbel[70], E. Golobardes[84], D. Golubkov[41], A. Golutvin[61,82], A. Gomes[1,a], S. Gomez Fernandez[45], F. Goncalves Abrantes[63], M. Goncerz[35], G. Gong[3], P. Gorbounov[41], I.V. Gorelov[40], C. Gotti[26], E. Govorkova[48], J.P. Grabowski[17], R. Graciani Diaz[45], T. Grammatico[13], L.A. Granado Cardoso[48], E. Graugés[45], E. Graverini[49], G. Graziani[22], A. Grecu[37], L.M. Greeven[32], P. Griffith[21,f], L. Grillo[62], S. Gromov[82], B.R. Gruberg Cazon[63], C. Gu[3], M. Guarise[21], P. A. Günther[17], E. Gushchin[39], A. Guth[14], Y. Guz[44,48], T. Gys[48], T. Hadavizadeh[69], G. Haefeli[49], C. Haen[48], J. Haimberger[48], T. Halewood-leagas[60], P.M. Hamilton[66], Q. Han[7], X. Han[17], T.H. Hancock[63], S. Hansmann-Menzemer[17], N. Harnew[63], T. Harrison[60], C. Hasse[48], M. Hatch[48], J. He[6,b], M. Hecker[61], K. Heijhoff[32], K. Heinicke[15], A.M. Hennequin[48], K. Hennessy[60], L. Henry[25,47], J. Heuel[14], A. Hicheur[2], D. Hill[49], M. Hilton[62], S.E. Hollitt[15], J. Hu[17], J. Hu[72], W. Hu[7], W. Huang[6], X. Huang[73], W. Hulsbergen[32], R.J. Hunter[56], M. Hushchyn[81], D. Hutchcroft[60], D. Hynds[32], P. Ibis[15], M. Idzik[34], D. Ilin[38], P. Ilten[65], A. Inglessi[38], A. Ishteev[82], K. Ivshin[38], R. Jacobsson[48], S. Jakobsen[48], E. Jans[32], B.K. Jashal[47], A. Jawahery[66], V. Jevtic[15], M. Jezabek[35], F. Jiang[3], M. John[63], D. Johnson[48], C.R. Jones[55], T.P. Jones[56], B. Jost[48], N. Jurik[48], S. Kandybei[51], Y. Kang[3], M. Karacson[48], M. Karpov[81], N. Kazeev[81], F. Keizer[55,48], M. Kenzie[56], T. Ketel[33], B. Khanji[15], A. Kharisova[83], S. Kholodenko[44], K.E. Kim[68], T. Kirn[14], V.S. Kirsebom[49], O. Kitouni[64], S. Klaver[32], K. Klimaszewski[36], S. Koliiev[52], A. Kondybayeva[82], A. Konoplyannikov[41], P. Kopciewicz[34], R. Kopecna[17], P. Koppenburg[32], M. Korolev[40], I. Kostiuk[32,52], O. Kot[52], S. Kotriakhova[38,30], P. Kravchenko[38], L. Kravchuk[39], R.D. Krawczyk[48], M. Kreps[56], F. Kress[61], S. Kretzschmar[14], P. Krokovny[43,v], W. Krupa[34], W. Krzemien[36], W. Kucewicz[35,t], M. Kucharczyk[35], V. Kudryavtsev[43,v], H.S. Kuindersma[32], G.J. Kunde[67], T. Kvaratskheliya[41], D. Lacarrere[48], G. Lafferty[62], A. Lai[27], A. Lampis[27], D. Lancierini[50], J.J. Lane[62], R. Lane[54], G. Lanfranchi[23], C. Langenbruch[14], J. Langer[15], O. Lantwin[50,82], T. Latham[56], F. Lazzari[29,q], R. Le Gac[10], S.H. Lee[85], R. Lefèvre[9], A. Leflat[40], S. Legotin[82], O. Leroy[10], T. Lesiak[35], B. Leverington[17], H. Li[72], L. Li[63], P. Li[17], Y. Li[4], Y. Li[4], Z. Li[68], X. Liang[68], T. Lin[61], R. Lindner[48], V. Lisovskyi[15], R. Litvinov[27], G. Liu[72], H. Liu[6], S. Liu[4], X. Liu[3], A. Loi[27], J. Lomba Castro[46], I. Longstaff[59], J.H. Lopes[2], G.H. Lovell[55], Y. Lu[4], D. Lucchesi[28,l], S. Luchuk[39], M. Lucio Martinez[32], V. Lukashenko[32], Y. Luo[3], A. Lupato[62], E. Luppi[21,f], O. Lupton[56], A. Lusiani[29,m], X. Lyu[6], L. Ma[4], R. Ma[6], S. Maccolini[20,d], F. Machefert[11], F. Maciuc[37], V. Macko[49], P. Mackowiak[15], S. Maddrell-Mander[54], O. Madejczyk[34], L.R. Madhan Mohan[54], O. Maev[38], A. Maevskiy[81], D. Maisuzenko[38], M.W. Majewski[34], J.J. Malczewski[35], S. Malde[63], B. Malecki[48], A. Malinin[80], T. Maltsev[43,v], H. Malygina[17], G. Manca[27,e], G. Mancinelli[10], R. Manera Escalero[45], D. Manuzzi[20,d], D. Marangotto[25,i], J. Maratas[9,s], J.F. Marchand[8], U. Marconi[20], S. Mariani[22,g,48], C. Marin Benito[11], M. Marinangeli[49], P. Marino[49,m], J. Marks[17], P.J. Marshall[60], G. Martellotti[30], L. Martinazzoli[48,j], M. Martinelli[26,j], D. Martinez Santos[46], F. Martinez Vidal[47], A. Massafferri[1], M. Materok[14], R. Matev[48], A. Mathad[50], Z. Mathe[48], V. Matiunin[41], C. Matteuzzi[26], K.R. Mattioli[85], A. Mauri[32], E. Maurice[12], J. Mauricio[45], M. Mazurek[36], M. McCann[61], L. Mcconnell[18], T.H. Mcgrath[62], A. McNab[62], R. McNulty[18], J.V. Mead[60], B. Meadows[65], C. Meaux[10], G. Meier[15], N. Meinert[76], D. Melnychuk[36], S. Meloni[26,j], M. Merk[32,79], A. Merli[25], L. Meyer Garcia[2], M. Mikhasenko[48], D.A. Milanes[74], E. Millard[56], M. Milovanovic[48], M.-N. Minard[8], L. Minzoni[21,f], S.E. Mitchell[58], B. Mitreska[62], D.S. Mitzel[48], A. Mödden [15], R.A. Mohammed[63], R.D. Moise[61], T. Mombächer[15], I.A. Monroy[74], S. Monteil[9], M. Morandin[28], G. Morello[23], M.J. Morello[29,m], J. Moron[34], A.B. Morris[75], A.G. Morris[56], R. Mountain[68], H. Mu[3], F. Muheim[58,48], M. Mukherjee[7], M. Mulder[48], D. Müller[48], K. Müller[50], C.H. Murphy[63], D. Murray[62], P. Muzzetto[27,48], P. Naik[54], T. Nakada[49], R. Nandakumar[57], T. Nanut[49], I. Nasteva[2], M. Needham[58], I. Neri[21], N. Neri[25,i], S. Neubert[75], N. Neufeld[48], R. Newcombe[61], T.D. Nguyen[49], C. Nguyen-Mau[49,x], E.M. Niel[11], S. Nieswand[14], N. Nikitin[40], N.S. Nolte[48], C. Nunez[85], A. Oblakowska-Mucha[34], V. Obraztsov[44], D.P. O'Hanlon[54], R. Oldeman[27,e], M.E. Olivares[68], C.J.G. Onderwater[78], A. Ossowska[35], J.M. Otalora Goicochea[2], T. Ovsiannikova[41], P. Owen[50], A. Oyanguren[47], B. Pagare[56], P.R. Pais[48], T. Pajero[29,m,48], A. Palano[19], M. Palutan[23], Y. Pan[62], G. Panshin[83], A. Papanestis[57], M. Pappagallo[19,c], L.L. Pappalardo[21,f], C. Pappenheimer[65], W. Parker[66], C. Parkes[62], C.J. Parkinson[46], B. Passalacqua[21], G. Passaleva[22], A. Pastore[19], M. Patel[61], C. Patrignani[20,d], C.J. Pawley[79], A. Pearce[48], A. Pellegrino[32], M. Pepe Altarelli[48], S. Perazzini[20], D. Pereima[41], P. Perret[9], K. Petridis[54], A. Petrolini[24,h], A. Petrov[80], S. Petrucci[58], M. Petruzzo[25], T.T.H. Pham[68], A. Philippov[42], L. Pica[29,n], M. Piccini[77], B. Pietrzyk[8], G. Pietrzyk[49], M. Pili[63], D. Pinci[30], F. Pisani[48], A. Piucci[17], Resmi P.K[10], V. Placinta[37], J. Plews[53], M. Plo Casasus[46], F. Polci[13], M. Poli Lener[23], M. Poliakova[68], A. Poluektov[10], N. Polukhina[82,u], I. Polyakov[68], E. Polycarpo[2], G.J. Pomery[54], S. Ponce[48], D. Popov[6,48], S. Popov[42], S. Poslavskii[44], K. Prasanth[35], L. Promberger[48], C. Prouve[46], V. Pugatch[52], H. Pullen[63], G. Punzi[29,n], W. Qian[6], J. Qin[6], R. Quagliani[13], B. Quintana[8], N.V. Raab[18], R.I. Rabadan Trejo[10], B. Rachwal[34], J.H. Rademacker[54], M. Rama[29], M. Ramos Pernas[56], M.S. Rangel[2], F. Ratnikov[42,81], G. Raven[33], M. Reboud[8], F. Redi[49], F. Reiss[13], C. Remon Alepuz[47], Z. Ren[3], V. Renaudin[63], R. Ribatti[29], S. Ricciardi[57], K. Rinnert[60], P. Robbe[11], A. Robert[13], G. Robertson[58], A.B. Rodrigues[49], E. Rodrigues[60], J.A. Rodriguez Lopez[74], A. Rollings[63], P. Roloff[48], V. Romanovskiy[44], M. Romero Lamas[46], A. Romero Vidal[46], J.D. Roth[85], M. Rotondo[23], M.S. Rudolph[68], T. Ruf[48], J. Ruiz Vidal[47], A. Ryzhikov[81], J. Ryzka[34], J.J. Saborido Silva[46], N. Sagidova[38], N. Sahoo[56], B. Saitta[27,e], D. Sanchez Gonzalo[45], C. Sanchez Gras[32], R. Santacesaria[30], C. Santamarina Rios[46], M. Santimaria[23], E. Santovetti[31,p], D. Saranin[82], G. Sarpis[59], M. Sarpis[75], A. Sarti[30], C. Satriano[30,o], A. Satta[31], M. Saur[15], D. Savrina[41,40], H. Sazak[9], L.G. Scantlebury Smead[63], S. Schael[14], M. Schellenberg[15], M. Schiller[59], H. Schindler[48], M. Schmelling[16], B. Schmidt[48], O. Schneider[49], A. Schopper[48], M. Schubiger[32], S. Schulte[49], M.H. Schune[11], R. Schwemmer[48], B. Sciascia[23], A. Sciubba[23], S. Sellam[46], A. Semennikov[41], M. Senghi Soares[33], A. Sergi[24,48], N. Serra[50], L. Sestini[28], A. Seuthe[15], P. Seyfert[48], D.M. Shangase[85], M. Shapkin[44], I. Shchemerov[82], L. Shchutska[49], T. Shears[60], L. Shekhtman[43,v], Z. Shen[5], V. Shevchenko[80], E.B. Shields[26,j], E. Shmanin[82], J.D. Shupperd[68], B.G. Siddi[21], R. Silva Coutinho[50], G. Simi[28], S. Simone[19,c], N. Skidmore[62], T. Skwarnicki[68], M.W. Slater[53], I. Slazyk[21,f], J.C. Smallwood[63], J.G. Smeaton[55], A. Smetkina[41], E. Smith[14], M. Smith[61], A. Snoch[32], M. Soares[20], L. Soares Lavra[9], M.D. Sokoloff[65], F.J.P. Soler[59], A. Solovev[38], I. Solovyev[38], F.L. Souza De Almeida[2], B. Souza De Paula[2], B. Spaan[15], E. Spadaro Norella[25,i], P. Spradlin[59], F. Stagni[48], M. Stahl[65], S. Stahl[48], P. Stefko[49], O. Steinkamp[50,82], S. Stemmle[17], O. Stenyakin[44], H. Stevens[15], S. Stone[68], M.E. Stramaglia[49], M. Straticiuc[37], D. Strekalina[82], F. Suljik[63], J. Sun[27], L. Sun[73], Y. Sun[66], P. Svihra[62], P.N. Swallow[53], K. Swientek[34], A. Szabelski[36], T. Szumlak[34], M. Szymanski[48], S. Taneja[62], F. Teubert[48], E. Thomas[48], K.A. Thomson[60], M.J. Tilley[61], V. Tisserand[9], S. T'Jampens[8], M. Tobin[4], S. Tolk[48], L. Tomassetti[21,f], D. Torres Machado[1], D.Y. Tou[13], M. Traill[59], M.T. Tran[49], E. Trifonova[82], C. Trippl[49], G. Tuci[29,n], A. Tully[49], N. Tuning[32,48], A. Ukleja[36], D.J. Unverzagt[17], E. Ursov[82], A. Usachov[32], A. Ustyuzhanin[42,81], U. Uwer[17], A. Vagner[83], V. Vagnoni[20], A. Valassi[48], G. Valenti[20], N. Valls Canudas[45], M. van Beuzekom[32], M. Van Dijk[49], E. van Herwijnen[82], C.B. Van Hulse[18], M. van Veghel[78], R. Vazquez Gomez[46], P. Vazquez Regueiro[46], C. Vázquez Sierra[48], S. Vecchi[21], J.J. Velthuis[54], M. Veltri[22,r], A. Venkateswaran[68], M. Veronesi[32], M. Vesterinen[56], D. Vieira[65], M. Vieites Diaz[49], H. Viemann[76], X. Vilasis-Cardona[84], E. Vilella Figueras[60], P. Vincent[13],

G. Vitali[29], A. Vollhardt[50], D. Vom Bruch[10], A. Vorobyev[38], V. Vorobyev[43,v], N. Voropaev[38], R. Waldi[76], J. Walsh[29], C. Wang[17], J. Wang[5], J. Wang[4], J. Wang[3], J. Wang[73], M. Wang[3], R. Wang[54], Y. Wang[7], Z. Wang[50], H.M. Wark[60], N.K. Watson[53], S.G. Weber[13], D. Websdale[61], C. Weisser[64], B.D.C. Westhenry[54], D.J. White[62], M. Whitehead[54], D. Wiedner[15], G. Wilkinson[63], M. Wilkinson[68], I. Williams[55], M. Williams[64,69], M.R.J. Williams[58], F.F. Wilson[57], W. Wislicki[36], M. Witek[35], L. Witola[17], G. Wormser[11], S.A. Wotton[55], H. Wu[68], K. Wyllie[48], Z. Xiang[6], D. Xiao[7], Y. Xie[7], A. Xu[5], J. Xu[6], L. Xu[3], M. Xu[7], Q. Xu[6], Z. Xu[5], Z. Xu[6], D. Yang[3], S. Yang[6], Y. Yang[6], Z. Yang[3], Z. Yang[66], Y. Yao[68], L.E. Yeomans[60], H. Yin[7], J. Yu[71], X. Yuan[68], O. Yushchenko[44], E. Zaffaroni[49], K.A. Zarebski[53], M. Zavertyaev[16,u], M. Zdybal[35], O. Zenaiev[48], M. Zeng[3], D. Zhang[7], L. Zhang[3], S. Zhang[5], Y. Zhang[5], Y. Zhang[63], A. Zhelezov[17], Y. Zheng[6], X. Zhou[6], Y. Zhou[6], X. Zhu[3], V. Zhukov[14,40], J.B. Zonneveld[58], S. Zucchelli[20,d], D. Zuliani[28], G. Zunica[62].

[1]*Centro Brasileiro de Pesquisas Físicas (CBPF), Rio de Janeiro, Brazil*
[2]*Universidade Federal do Rio de Janeiro (UFRJ), Rio de Janeiro, Brazil*
[3]*Center for High Energy Physics, Tsinghua University, Beijing, China*
[4]*Institute Of High Energy Physics (IHEP), Beijing, China*
[5]*School of Physics State Key Laboratory of Nuclear Physics and Technology, Peking University, Beijing, China*
[6]*University of Chinese Academy of Sciences, Beijing, China*
[7]*Institute of Particle Physics, Central China Normal University, Wuhan, Hubei, China*
[8]*Univ. Savoie Mont Blanc, CNRS, IN2P3-LAPP, Annecy, France*
[9]*Université Clermont Auvergne, CNRS/IN2P3, LPC, Clermont-Ferrand, France*
[10]*Aix Marseille Univ, CNRS/IN2P3, CPPM, Marseille, France*
[11]*Université Paris-Saclay, CNRS/IN2P3, IJCLab, Orsay, France*
[12]*Laboratoire Leprince-Ringuet, CNRS/IN2P3, Ecole Polytechnique, Institut Polytechnique de Paris, Palaiseau, France*
[13]*LPNHE, Sorbonne Université, Paris Diderot Sorbonne Paris Cité, CNRS/IN2P3, Paris, France*
[14]*I. Physikalisches Institut, RWTH Aachen University, Aachen, Germany*
[15]*Fakultät Physik, Technische Universität Dortmund, Dortmund, Germany*
[16]*Max-Planck-Institut für Kernphysik (MPIK), Heidelberg, Germany*
[17]*Physikalisches Institut, Ruprecht-Karls-Universität Heidelberg, Heidelberg, Germany*
[18]*School of Physics, University College Dublin, Dublin, Ireland*
[19]*INFN Sezione di Bari, Bari, Italy*
[20]*INFN Sezione di Bologna, Bologna, Italy*
[21]*INFN Sezione di Ferrara, Ferrara, Italy*
[22]*INFN Sezione di Firenze, Firenze, Italy*
[23]*INFN Laboratori Nazionali di Frascati, Frascati, Italy*
[24]*INFN Sezione di Genova, Genova, Italy*
[25]*INFN Sezione di Milano, Milano, Italy*
[26]*INFN Sezione di Milano-Bicocca, Milano, Italy*
[27]*INFN Sezione di Cagliari, Monserrato, Italy*
[28]*Universita degli Studi di Padova, Universita e INFN, Padova, Padova, Italy*
[29]*INFN Sezione di Pisa, Pisa, Italy*
[30]*INFN Sezione di Roma La Sapienza, Roma, Italy*
[31]*INFN Sezione di Roma Tor Vergata, Roma, Italy*
[32]*Nikhef National Institute for Subatomic Physics, Amsterdam, Netherlands*
[33]*Nikhef National Institute for Subatomic Physics and VU University Amsterdam, Amsterdam, Netherlands*
[34]*AGH - University of Science and Technology, Faculty of Physics and Applied Computer Science, Kraków, Poland*
[35]*Henryk Niewodniczanski Institute of Nuclear Physics Polish Academy of Sciences, Kraków, Poland*
[36]*National Center for Nuclear Research (NCBJ), Warsaw, Poland*
[37]*Horia Hulubei National Institute of Physics and Nuclear Engineering, Bucharest-Magurele, Romania*
[38]*Petersburg Nuclear Physics Institute NRC Kurchatov Institute (PNPI NRC KI), Gatchina, Russia*

[39] Institute for Nuclear Research of the Russian Academy of Sciences (INR RAS), Moscow, Russia
[40] Institute of Nuclear Physics, Moscow State University (SINP MSU), Moscow, Russia
[41] Institute of Theoretical and Experimental Physics NRC Kurchatov Institute (ITEP NRC KI), Moscow, Russia
[42] Yandex School of Data Analysis, Moscow, Russia
[43] Budker Institute of Nuclear Physics (SB RAS), Novosibirsk, Russia
[44] Institute for High Energy Physics NRC Kurchatov Institute (IHEP NRC KI), Protvino, Russia, Protvino, Russia
[45] ICCUB, Universitat de Barcelona, Barcelona, Spain
[46] Instituto Galego de Física de Altas Enerxías (IGFAE), Universidade de Santiago de Compostela, Santiago de Compostela, Spain
[47] Instituto de Fisica Corpuscular, Centro Mixto Universidad de Valencia - CSIC, Valencia, Spain
[48] European Organization for Nuclear Research (CERN), Geneva, Switzerland
[49] Institute of Physics, Ecole Polytechnique Fédérale de Lausanne (EPFL), Lausanne, Switzerland
[50] Physik-Institut, Universität Zürich, Zürich, Switzerland
[51] NSC Kharkiv Institute of Physics and Technology (NSC KIPT), Kharkiv, Ukraine
[52] Institute for Nuclear Research of the National Academy of Sciences (KINR), Kyiv, Ukraine
[53] University of Birmingham, Birmingham, United Kingdom
[54] H.H. Wills Physics Laboratory, University of Bristol, Bristol, United Kingdom
[55] Cavendish Laboratory, University of Cambridge, Cambridge, United Kingdom
[56] Department of Physics, University of Warwick, Coventry, United Kingdom
[57] STFC Rutherford Appleton Laboratory, Didcot, United Kingdom
[58] School of Physics and Astronomy, University of Edinburgh, Edinburgh, United Kingdom
[59] School of Physics and Astronomy, University of Glasgow, Glasgow, United Kingdom
[60] Oliver Lodge Laboratory, University of Liverpool, Liverpool, United Kingdom
[61] Imperial College London, London, United Kingdom
[62] Department of Physics and Astronomy, University of Manchester, Manchester, United Kingdom
[63] Department of Physics, University of Oxford, Oxford, United Kingdom
[64] Massachusetts Institute of Technology, Cambridge, MA, United States
[65] University of Cincinnati, Cincinnati, OH, United States
[66] University of Maryland, College Park, MD, United States
[67] Los Alamos National Laboratory (LANL), Los Alamos, United States
[68] Syracuse University, Syracuse, NY, United States
[69] School of Physics and Astronomy, Monash University, Melbourne, Australia, associated to [56]
[70] Pontifícia Universidade Católica do Rio de Janeiro (PUC-Rio), Rio de Janeiro, Brazil, associated to [2]
[71] Physics and Micro Electronic College, Hunan University, Changsha City, China, associated to [7]
[72] Guangdong Provencial Key Laboratory of Nuclear Science, Institute of Quantum Matter, South China Normal University, Guangzhou, China, associated to [3]
[73] School of Physics and Technology, Wuhan University, Wuhan, China, associated to [3]
[74] Departamento de Fisica , Universidad Nacional de Colombia, Bogota, Colombia, associated to [13]
[75] Universität Bonn - Helmholtz-Institut für Strahlen und Kernphysik, Bonn, Germany, associated to [17]
[76] Institut für Physik, Universität Rostock, Rostock, Germany, associated to [17]
[77] INFN Sezione di Perugia, Perugia, Italy, associated to [21]
[78] Van Swinderen Institute, University of Groningen, Groningen, Netherlands, associated to [32]
[79] Universiteit Maastricht, Maastricht, Netherlands, associated to [32]
[80] National Research Centre Kurchatov Institute, Moscow, Russia, associated to [41]
[81] National Research University Higher School of Economics, Moscow, Russia, associated to [42]
[82] National University of Science and Technology "MISIS", Moscow, Russia, associated to [41]
[83] National Research Tomsk Polytechnic University, Tomsk, Russia, associated to [41]
[84] DS4DS, La Salle, Universitat Ramon Llull, Barcelona, Spain, associated to [45]
[85] University of Michigan, Ann Arbor, United States, associated to [68]

[a] Universidade Federal do Triângulo Mineiro (UFTM), Uberaba-MG, Brazil
[b] Hangzhou Institute for Advanced Study, UCAS, Hangzhou, China
[c] Università di Bari, Bari, Italy
[d] Università di Bologna, Bologna, Italy
[e] Università di Cagliari, Cagliari, Italy

[f] *Università di Ferrara, Ferrara, Italy*
[g] *Università di Firenze, Firenze, Italy*
[h] *Università di Genova, Genova, Italy*
[i] *Università degli Studi di Milano, Milano, Italy*
[j] *Università di Milano Bicocca, Milano, Italy*
[k] *Università di Modena e Reggio Emilia, Modena, Italy*
[l] *Università di Padova, Padova, Italy*
[m] *Scuola Normale Superiore, Pisa, Italy*
[n] *Università di Pisa, Pisa, Italy*
[o] *Università della Basilicata, Potenza, Italy*
[p] *Università di Roma Tor Vergata, Roma, Italy*
[q] *Università di Siena, Siena, Italy*
[r] *Università di Urbino, Urbino, Italy*
[s] *MSU - Iligan Institute of Technology (MSU-IIT), Iligan, Philippines*
[t] *AGH - University of Science and Technology, Faculty of Computer Science, Electronics and Telecommunications, Kraków, Poland*
[u] *P.N. Lebedev Physical Institute, Russian Academy of Science (LPI RAS), Moscow, Russia*
[v] *Novosibirsk State University, Novosibirsk, Russia*
[w] *Department of Physics and Astronomy, Uppsala University, Uppsala, Sweden*
[x] *Hanoi University of Science, Hanoi, Vietnam*